Nitrite oxidation exceeds reduction and fixed nitrogen loss in anoxic Pacific waters

Andrew R. Babbin[a,*], Carolyn Buchwald[b,c], François M.M. Morel[d], Scott D. Wankel[b], Bess B. Ward[d]

[a] *Department of Earth, Atmospheric, and Planetary Sciences, Massachusetts Institute of Technology, Cambridge, Massachusetts 02139, USA*
[b] *Department of Marine Chemistry and Geochemistry, Woods Hole Oceanographic Institution, Woods Hole, Massachusetts 02543, USA*
[c] *Department of Oceanography, Dalhousie University, Halifax, Nova Scotia B3H 4R2, Canada*
[d] *Department of Geosciences, Princeton University, Princeton, New Jersey 08544, USA*

ABSTRACT

The diversity of nitrogen-based dissimilatory metabolisms in anoxic waters continues to increase with additional studies to the marine oxygen deficient zones (ODZs). Although the microbial oxidation of nitrite (NO_2^-) has been known for over a century, studies of the pathways and microbes involved have generally proceeded under the assumption that nitrite oxidation to nitrate requires dioxygen (O_2). Anaerobic NO_2^- oxidation until now has been conclusively shown only for anammox bacteria, albeit only as a limited sink for NO_2^- in their metabolism compared to the NO_2^- reduced to N_2. Here, using direct experimental techniques optimized for replicating in situ anoxic conditions, we show that NO_2^- oxidation is substantial, widespread, and consistent across the ODZs of the eastern tropical Pacific Ocean. Regardless of the specific oxidant, NO_2^- oxidation rates are up to an order of magnitude larger than simultaneous N_2 production rates for which these zones are known, and cannot be explained by anammox rates alone. Higher rates of NO_2^- oxidation over reduction in anoxic waters are paradoxical but help to explain how anammox rates can be enhanced over denitrification in shallow anoxic waters ($\sigma_\theta < 26.4$) at the edge of the ODZs but not within the ODZ core. Furthermore, nitrite oxidation may be the key to reconciliation of the perceived imbalance of the global fixed nitrogen loss budget.

1. Introduction

The inventory of fixed, i.e. biologically available, nitrogen (N) limits the productivity of much of the world's oceans, and in turn significantly feeds back on Earth's climate through its coupling to the carbon cycle. The loss of fixed N occurs exclusively at O_2 concentrations less than 1% of saturation (Codispoti, 2007; Dalsgaard et al., 2014; Babbin et al., 2014). In ocean waters, this regime is restricted to the functionally anoxic O_2 deficient zones (ODZs) of the eastern tropical Pacific (ETP) and the Arabian Sea. Together these regions comprise less than 0.1% of the ocean's volume but account for the entirety of water column fixed N loss (Codispoti, 2007). The pathways responsible for this loss – denitrification and anammox – are mediated by microorganisms subsisting anaerobically, at O_2 concentrations < 10 nmol L^{-1} (Revsbech et al., 2009).

Attribution of the relative importance of N_2 production processes, i.e., denitrification vis-à-vis anammox, has been the subject of intense debate since the discovery of anammox in the marine environment nearly 20 years ago (Thamdrup and Dalsgaard, 2002; Dalsgaard et al., 2003; Lam et al., 2009; Ward et al., 2009). In ODZs, NO_3^-, the most oxidized and abundant fixed N species, is reduced to inert N_2 gas via either (i) heterotrophic denitrification through intermediate NO_2^- and gaseous species, or (ii) anammox whereby autotrophic organisms use NO_2^- to oxidize ammonium, which is released in situ as a byproduct of heterotrophy. An overall balanced loss, that is, a denitrification to anammox ratio such that ammonium production by organic N remineralization stoichiometrically balances ammonium consumption by anammox, might be a system level constraint (Dalsgaard et al., 2012; Babbin et al., 2014), but this consistency of ~70% denitrification is rarely observed at the sub-liter scale of individual measurements. Instead, anammox is frequently found to dominate the nitrogen loss budget, e.g., (Hamersley et al., 2007; Lam et al., 2009), but the source of the ammonium necessary for this metabolism remains a mystery.

Experimental evidence from the Eastern Tropical South Pacific ODZ suggests a rapid cycling between NO_3^- and NO_2^-, with iodate as a potential NO_2^- oxidant (Peters et al., 2016; Babbin et al., 2017).

---

* Corresponding author.
E-mail address: babbin@mit.edu (A.R. Babbin).

Moreover, NO_3^- reduction and NO_2^- oxidation rates have both been observed to be much faster than those of N_2 production, implying nitrate reduction does not proceed all the way to N_2 gas, e.g., (Füssel et al., 2011; Kalvelage et al., 2013; Babbin et al., 2017). NO_2^- may be the overlooked critical intermediate for balancing the observed anammox and denitrification rates in the ODZs. The denitrification pathway has classically been considered as the full and linked stepwise reductions from NO_3^- to NO_2^-, NO, N_2O, and N_2. In cultures and wastewater reactors, however, denitrifying organisms capable of full NO_3^- reduction to N_2O and N_2 tend to initially reduce NO_3^- to NO_2^-, allowing NO_2^- to build up before expressing the genes for further NO_2^- reduction (Betlach and Tiedje, 1981). Additionally, reports from multiple ODZs show in situ NO_3^- reduction rates to be much faster than NO_2^- reduction (Lam et al., 2009, 2011; Füssel et al., 2011; Kalvelage et al., 2013). This metabolic imbalance on NO_2^- implies there is a pathway for NO_2^- consumption other than denitrification and anammox.

2. Nitrite oxidation within ODZs

Evidence for one such nitrite sink, NO_2^- oxidation, has been presented in the ETP from the few studies that have investigated it directly using tracer techniques (Lipschultz et al., 1990; Füssel et al., 2011; Kalvelage et al., 2015; Peng et al., 2015, 2016). NO_2^- oxidation remains largely ignored when calculating the N budget in ODZs, however. The data indicate fast rates for the ODZs, on order of 100 nmol L^{-1} d^{-1}, but they are limited and may be biased by selective sampling and experimental complications. While those data are intriguing, they are almost entirely confined to the overlying oxygenated waters, with few measurements in the anoxic core and even fewer at the anoxic boundary (Lipschultz et al., 1990; Beman et al., 2013; Peng et al., 2016). Resolving the inconsistency across studies, specifically whether NO_2^- oxidation peaks in the boundary waters at the interface between the oxygenated and anoxic depths or within the core of the ODZ, necessitates more measurements at higher vertical resolution.

Studies analyzing natural abundance N and O isotope ratios also imply significant NO_2^- oxidation in the ETP, especially at the boundaries (Sigman et al., 2005; Casciotti et al., 2013; Buchwald et al., 2015; Peters et al., 2016). While these types of measurements do not suffer from the same artifacts as tracer incubations, natural abundance isotopes provide integrated measures that do not require NO_2^- oxidation to occur in situ in the absence of O_2. In fact, proposals regarding the dynamic injection of O_2 into anoxic depths (Casciotti et al., 2013) or trace O_2 levels (Tsementzi et al., 2016; Bristow et al., 2017) have been invoked to explain the NO_2^- oxidation implied by the isotopic evidence. Although NO_2^- oxidizers have been considered to be obligately aerobic (Lees and Simpson, 1957), the actual oxidation reaction does not require molecular O_2; even in aerobic cultures, the additional oxygen atom in NO_3^- is derived from water (DiSpirito and Hooper, 1986).

Here we address several issues outlined above – the sparse data, the lack of consensus regarding the magnitude and vertical distribution of NO_2^- oxidation rates within the ODZ, and the absence of a reasonable mass balance on the fixed N budget by exploring all possible anaerobic NO_2^- consumption pathways, both reduction to N_2 and oxidation to NO_3^- using data from multiple expeditions in the ETP. We further link these nitrite oxidation data to a compendium of depth-resolved anammox and denitrification rates to show the relationship between nitrite oxidation and the enhancement of anammox rates over denitrification.

3. Methods

3.1. Sample collection and onboard rate incubations

Sampling and incubations were conducted onboard the *R/V Thomas G. Thompson* cruise TN278 in March and April 2012 in the ETNP, and onboard the *RVIB Nathaniel B. Palmer* cruise NBP1305 in June and July 2013 in the ETSP using methods as previously described (Babbin et al.,
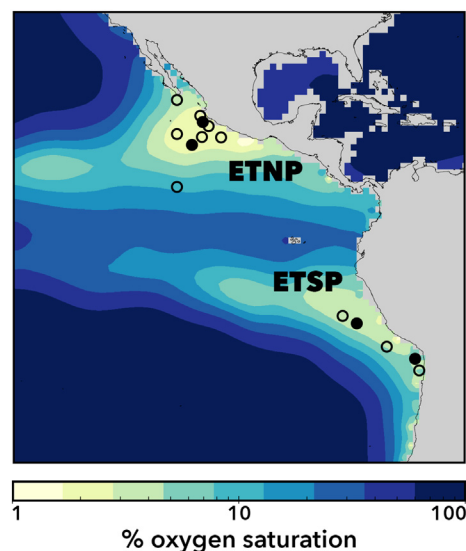

Fig. 1. Station map of sampling locations. Locations from which samples were collected for only N_2 production at 4 depths are shown by the open circles; those sampled at 8 depths for N_2 production and NO_2^- oxidation are shown by filled circles. Color contours represent the oxygen saturation percentage of the depth layer centered about 200 m, from World Ocean Atlas 2018 (Garcia et al., 2018).

2014, 2015). Water from 8 depths at 2 stations each in the Eastern Tropical North and South Pacific (ETNP and ETSP, respectively; Fig. 1) was carefully collected to resolve vertical profiles of anammox, denitrification, and nitrite oxidation through the anoxic layer. Water from 4 depths each at multiple additional stations in both basins was further collected for only anammox and denitrification rates. The top of the ODZ, where the most intense cycling and fastest microbial rates occur (Kalvelage et al., 2013; Babbin et al., 2014), was sampled at the highest resolution. Targeted depths were sampled using Niskin bottles within the oxycline and core of anoxic waters from each station (Table 1). The core, functionally anoxic, ODZ was identified as the depths where the Seabird SBE43 Clark-style O_2 electrode achieved its minimal signal and no vertical gradient in O_2 was observed, and confirmed by STOX electrode measurements on the CTD (Tiano et al., 2014; Garcia-Robledo et al., 2017). Seawater was mostly collected from anoxic depths using techniques developed to remove O_2 contamination (Thamdrup and Dalsgaard, 2002; Ward et al., 2009; Babbin et al., 2014; De Brabandere et al., 2014), amended with isotope tracer, aliquoted into fifteen 12 mL sample vials (Exetainer, Labco, UK), purged with helium, and incubated near in situ temperature (10°C) in the dark. At time intervals of 8–12 h, triplicate samples were preserved with a 50 μL injection of 7 mol L^{-1} zinc chloride. Bubbling samples with helium also notably removes the trace intermediate gases in denitrification (NO and N_2O), but because their concentrations are so low (Ward and Zafirou, 1988; Babbin et al., 2015; Ji et al., 2015), they would be reestablished within a couple

Table 1
Characteristics of sampling sites.

Station	ETNP coastal	ETNP offshore	ETSP coastal	ETSP offshore
Latitude / Longitude	20° 00′ N 106° 00′ W	16° 31′ N 107° 06′ W	20° 40′ S 70° 41′ W	13° 57′ S 81° 14′ W
Depth chl. max (m)	15	105	20	40
Top ODZ (m)	40	115	80	175
Chl. max (μg/L)	29	3.6	1.8	1.4

Location, depths of chlorophyll (chl) maximum and onset of oxygen deficient zone (ODZ; $O_2 < 10$ nmol L^{-1}), and concentration of chlorophyll at the chlorophyll maximum are provided for each of the 4 study sites.

hours.

Exacting care was taken in the preparation of the incubation vials. First, Niskin bottles were sampled directly into borosilicate flasks with precision ground glass stoppered caps designed to eliminate gas exchange and widely used for dissolved oxygen analysis and the storage of certified inorganic carbon reference standards for years. The bottles were overflowed with seawater, filled laminarly from the bottom for a minimum of four volume transfers. Bottles were stored at 10°C for at most 1 hour prior to the start of the incubations. The bottles were opened in a portable N_2-filled glove bag that was flushed and evacuated three times before a final fill. Each individual Exetainer vial was flushed directly before filling with sample. Positive pressure was maintained at all times in the bag by maintaining a slow bleed of gas into the bag. The Exetainer caps with septa were stored in an anaerobic GasPak culturing vessel (Becton, Dickinson and Co., USA) flushed with helium and vacuumed three times, and also filled with oxygen-reactive catalyst to remove contaminant oxygen for at least 1 month. The chamber was only opened in a N_2-flushed globe bag following the same protocol as the incubations. After Exetainer vials were filled and capped, they were purged on an ultrahigh purity helium line for 5 minutes, amounting to 50 volume transfers. Carbon system parameters were confirmed to have minimal effect on pH over this short purge time due to the slow equilibration kinetics of the carbonate system compared with dissolved oxygen.

For the 4-depth stations, the rates of N_2 production were determined via a set of five contemporaneous incubation amendments: (A) $^{15}NO_2^-$ alone, (B) $^{15}NO_2^-$ + $^{14}NH_4^+$, (C) $^{15}NH_4^+$ alone, (D) $^{15}NH_4^+$ + $^{14}NO_2^-$, and (E) ($^{15}N)_2O$. These were designed to provide distinct rates of anammox (from the labeled ammonium and nitrite treatments) and denitrification (from the nitrite and nitrous oxide treatments) while also ensuring the organisms were not limited for other nitrite substrates (Ward et al., 2009; Bulow et al., 2010). The amendments for all compounds other than the $^{46}N_2O$ was 3 μmol L^{-1} whereas the $^{46}N_2O$ amendment was 30 nmol L^{-1} (Babbin et al., 2015).

For the 8-depth stations, the rates of NO_2^- transformation to both N_2 and NO_3^- by the in situ microbial community were quantified over 36–48 hour incubations using the stable isotope tracer $^{15}NO_2^-$. Given that NO_2^- reduction to N_2 requires very low O_2 concentrations (Babbin et al., 2014; Dalsgaard et al., 2014), the detection – in the same vials – of $^{15}N_2$ and $^{15}NO_3^-$ derived from $^{15}NO_2^-$ assured that any potential NO_2^- oxidation occurred with minimal contamination by O_2. Further, immediately and consistently linear NO_3^- production (Fig. 2) indicated the microbes were well adapted to and operating under anaerobic conditions in situ. Our experiments were contaminated by the same $^{15}NO_3^-$ artifact seen previously (Sun et al., 2017), but this artifact does not interfere with our rate determinations. Based on the initial $^{15}NO_3^-$ measurements for our different depths and stations, we were able to estimate a "contamination" artifact of ~2%, i.e., 2% of the $^{15}NO_x^-$ pool is not removed by sulfamic acid (Supplementary Fig. 1). This contamination has several potential sources: incomplete removal of NO_2^-, contamination in the NO_2^- tracer stock, and/or equilibration between NO_3^- and NO_2^- at the beginning of the experiment (Brunner et al., 2013; Kemeny et al., 2016). While the initial labeling in the $^{15}NO_3^-$ pool swamped the natural abundance signal (Fig. 2), this offset affects all vials within an incubation set equally as they all begin from the same mixed stock and seawater. The offset thus has no effect on the slope of $^{15}NO_3^-$ production over the time course, only the intercept (which is not part of the rate calculation equation). Previous NO_2^- oxidation measurements that assume no initial labeling can be revisited and corrected, however, based on their own in situ NO_3^- and NO_2^- concentrations, and stock solutions (akin to Supplementary Fig. 1).

3.2. Isotope analysis for nitrogen cycling rates

Production of $^{15}N_2$ from tracer additions was measured as previously, using standard gas chromatography/isotope ratio mass
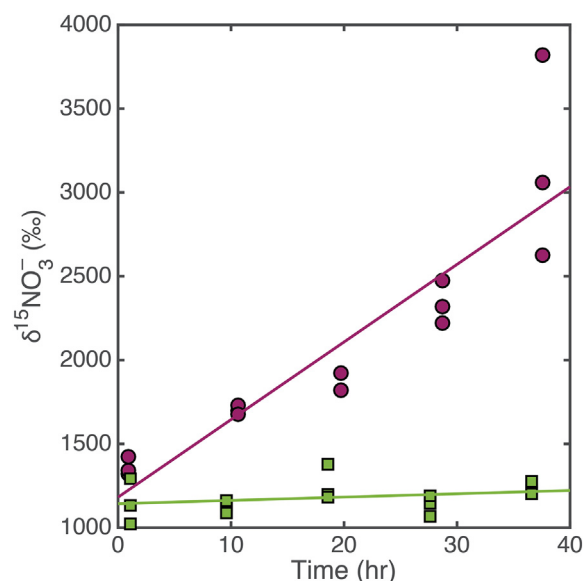

Fig. 2. Production of $^{15}NO_3^-$ from $^{15}NO_2^-$ tracer incubations with time. The linear production of heavy nitrate is shown for two depths (50 m, purple; 100 m, green) from the ETNP coastal site. The intercept initial label exceeding 1000‰ indicates a methodological offset (Fig. S1), albeit one that affects all samples equally given that each of the 15 vials sampled over time (representing 1 incubation) began with the same in situ and amended tracer concentrations. (For interpretation of the references to color in this figure legend, the reader is referred to the web version of this article.)

spectrometry methods (Europa 20/20) (Babbin et al., 2014). After mass spectrometer analysis of the gaseous products, $^{15}NO_3^-$ production in the same vials was determined using the denitrifier method (Sigman et al., 2001). In order to remove the remaining $^{15}NO_2^-$ in the incubation vials, concentrated sulfamic acid was added directly to the vials and allowed to react for 1 hour before restoring the pH to neutral with sodium hydroxide (Granger and Sigman, 2009). A volume of sample was injected into N_2-purged vials containing the washed cell suspensions of the denitrifier *Pseudomonas aureofaciens* such that 20 nmol NO_3^- were quantitatively converted to 10 nmol N_2O for measurement on an Isoprime 100 isotope ratio mass spectrometer.

3.3. Comparison of ETSP metagenome with Methylomirabilis oxyfera genome

A previously published metagenome (Ganesh et al., 2014) from the ETSP was compared with the quinol nitric oxide reductase paralogs identified by Ettwig et al. (2012) as possible nitric oxide dismutases using the National Center for Biotechnology Information (NCBI) standard nucleotide basic local alignment search tool (BLASTn) algorithm (http://blast.ncbi.nlm.nih.gov/) (Table 2). The proteins identified by Ettwig et al. (2012) were DAMO1889, DAMO2434, and DAMO2437, but they found DAMO1889 to be expressed only in low amounts, whereas the other two were among the most abundant gene transcripts and translated proteins in their *M. oxyfera* enrichment culture (Ettwig et al., 2012).

4. Results and discussion

4.1. Relative magnitudes of anammox and denitrification rates

Across the two occupations, 72 independent anammox and denitrification rates were determined from 14 stations (9 in the ETNP and 5 in the ETSP) via a combination of five different tracer amendments. The rates of anammox and denitrification determined from each of the amendment types are not significantly different from each other, or

Table 2
Putative NO dismutase BLAST hits from the ETSP.

Query ID	Subject sequence ID	Depth (m)	Size fraction (μm)	Identity %	Alignment length	E value	Score
DAMO 2437	gnl|SRA|SRR961675.5239.2	110	> 1.6	74.40	418	3.57E-63	248
	gnl|SRA|SRR961677.203001.2	200	> 1.6	75.54	278	1.98E-47	196
	gnl|SRA|SRR961675.74899.2	110	> 1.6	75.91	303	6.90E-47	194
	gnl|SRA|SRR961677.22435.2	200	> 1.6	72.52	302	2.25E-40	172
	gnl|SRA|SRR961677.53775.2	200	> 1.6	72.43	301	2.75E-39	168
	gnl|SRA|SRR961673.6006.2	110	0.22 – 1.6	71.58	285	3.13E-32	145
	gnl|SRA|SRR961677.202537.2	200	> 1.6	77.63	152	3.58E-25	122
	gnl|SRA|SRR961677.107476.2	200	> 1.6	74.87	191	3.58E-25	122
	gnl|SRA|SRR961673.49819.2	110	0.22 – 1.6	68.27	353	3.58E-25	122
	gnl|SRA|SRR961673.194309.2	110	0.22 – 1.6	71.31	237	4.36E-24	118
	gnl|SRA|SRR961673.191578.2	110	0.22 – 1.6	73.63	182	2.75E-20	105
	gnl|SRA|SRR961673.218407.2	110	0.22 – 1.6	73.48	181	9.59E-20	104
	gnl|SRA|SRR961677.86164.2	200	> 1.6	77.52	129	3.35E-19	102
	gnl|SRA|SRR961677.93218.2	200	> 1.6	78.45	116	1.42E-17	96.9
	gnl|SRA|SRR961676.114339.2	200	0.22 – 1.6	72.11	147	1.09E-12	80.6
	gnl|SRA|SRR961673.110894.2	110	0.22 – 1.6	76.92	104	1.09E-12	80.6
DAMO 2434	gnl|SRA|SRR961675.5239.2	110	> 1.6	76.01	421	7.34E-72	277
	gnl|SRA|SRR961675.74899.2	110	> 1.6	76.80	306	6.03E-54	217
	gnl|SRA|SRR961677.203001.2	200	> 1.6	75.54	278	1.97E-47	196
	gnl|SRA|SRR961677.22435.2	200	> 1.6	72.19	302	9.56E-39	167
	gnl|SRA|SRR961677.53775.2	200	> 1.6	72.09	301	3.34E-38	165
	gnl|SRA|SRR961673.6006.2	110	0.22 – 1.6	73.43	286	1.16E-37	163
	gnl|SRA|SRR961677.107476.2	200	> 1.6	77.55	196	2.57E-33	149
	gnl|SRA|SRR961673.194309.2	110	0.22 – 1.6	70.89	237	1.85E-22	113
	gnl|SRA|SRR961673.191578.2	110	0.22 – 1.6	73.08	182	1.17E-18	100
	gnl|SRA|SRR961673.218407.2	110	0.22 – 1.6	72.93	181	4.07E-18	98.7
	gnl|SRA|SRR961676.114339.2	200	0.22 – 1.6	72.86	140	3.13E-13	82.4
	gnl|SRA|SRR961676.17622.2	200	0.22 – 1.6	71.17	163	3.81E-12	78.8
	gnl|SRA|SRR961673.110894.2	110	0.22 – 1.6	75.47	106	4.64E-11	75.2

BLAST hits from the NCBI database using the sequences from Ettwig et al. (2012) putative dismutase sequences against the Ganesh et al. (2014) ETSP metagenome. Significant hits are defined as E-value $< 10^{-10}$ and Score > 75.

offset systematically (Babbin, Ph.D. thesis). As such, the mean and standard deviation of the rates determined from the compendium of tracer additions is used in this analysis, with denitrification determined from the $^{15}NO_2^- \pm ^{14}NH_4^+$ and $^{46}N_2O$ experiments and anammox from the $^{15}NH_4^+ \pm ^{14}NO_2^-$ and $^{15}NO_2^- \pm ^{14}NH_4^+$ experiments. Interestingly, because of no systematic offset between rates amended with and without unlabeled tracer, this set of incubations shows that anammox and denitrification were not limited by nitrite or ammonium at the time of sampling.

The rates of fixed nitrogen loss tended to be < 10 nmol L^{-1} d^{-1}, with the fraction of nitrogen loss attributed to anammox, as seen previously by other workers, generally higher than the predicted 30% (Fig. 3). However, a difference can be observed between the data from the shallowest depths and those within the core of the ODZ: in the core, defined by $\sigma_\theta > 26.4$, the fraction of anammox is not significantly different from the 30% expected partition, with the ETNP and ETSP, respectively exhibiting $39 \pm 5\%$ (se) and $41 \pm 3\%$ anammox. In the upper ODZ, however, anammox is enhanced, accounting for $52 \pm 4\%$ and $76 \pm 8\%$ in the ETNP and ETSP, respectively. Indeed, the shallow depths host substantially greater anammox relative to denitrification than their deeper counter parts (t statistic < 0.025). Interestingly, the shallowest samples, those outside of the canonical ODZ based on oxygen concentrations, exhibit enhanced denitrification over anammox albeit at very low rates (Fig. 4). This observation runs counter to the generally accepted paradigm that anammox is less inhibited by oxygen than denitrification (Babbin et al., 2014; Dalsgaard et al., 2014). This result might be explained by denitrification occurring in particle microenvironments (Ganesh et al., 2014; Bianchi et al., 2018), especially as these depths coincide with an observed accumulation of ammonium. Strikingly. across the full dataset, the variation in the fraction of N_2 loss attributed to anammox is due to the deviation in the rate of anammox rather than that of denitrification (Fig. 5).

4.2. Simultaneous measurements of NO_2^- oxidation and reduction rates

The depth-resolved profiles of NO_2^- oxidation rates observed at all four sites are remarkably consistent (Figs. 6–9). The shallowest samples, within the slightly oxygenated oxycline (visible in Figs. 6, 8), exhibit low rates before peaking in the uppermost anoxic layer. The microorganisms contained in the shallow oxycline community are consistently exposed to O_2 concentrations $\geq 10\%$ saturation, which is sufficient to allow many known obligate aerobic reactions to occur (Martens-Habbena et al., 2009; Tiano et al., 2014). These organisms are undoubtedly suited for life at some O_2 concentration greater than zero, and once the available O_2 was removed methodologically, they could not oxidize NO_2^-, even if another oxidant was available.

The highest rates of NO_2^- oxidation occurred in samples collected at the shallowest anoxic depths and reached up to 200 nmol L^{-1} d^{-1}. NO_2^- oxidation rates were up to an order of magnitude greater than the rates of NO_2^- reduction to N_2, which also peaked in the shallowest anoxic depths. These biological processes ultimately depend on organic matter flux derived from surface productivity (Kalvelage et al., 2013; Babbin et al., 2014, 2015) because the NO_2^- is supplied by in situ heterotrophy (i.e. NO_3^- respiration). During sampling, the coastal and ETNP sites exhibited higher chlorophyll concentrations, implying greater primary production, than the offshore and ETSP sites (Table 1), corresponding with the observed relative magnitudes in peak nitrite oxidation rates. Within the core of the ODZs, rates were lower, averaging 5.6 ± 1.4 (se) nmol L^{-1} d^{-1} across all stations, but generally still detectable. At the only site (coastal ETSP) where samples were collected from the bottom of the ODZ, the rates were again high at the lower oxic/anoxic boundary (Fig. 7). These substantial NO_2^- oxidation rates generally cannot be supported by NO_2^- oxidation conducted by anammox bacteria in their fixation of carbon by conventional stoichiometries (Strous et al., 1998). Our data show anammox accounts for $< 10\%$ of any NO_2^- oxidation rate measurement, averaging 3.4% (Supplementary Table 1). Careful consideration of the methodology minimizes O_2 as a controlling factor
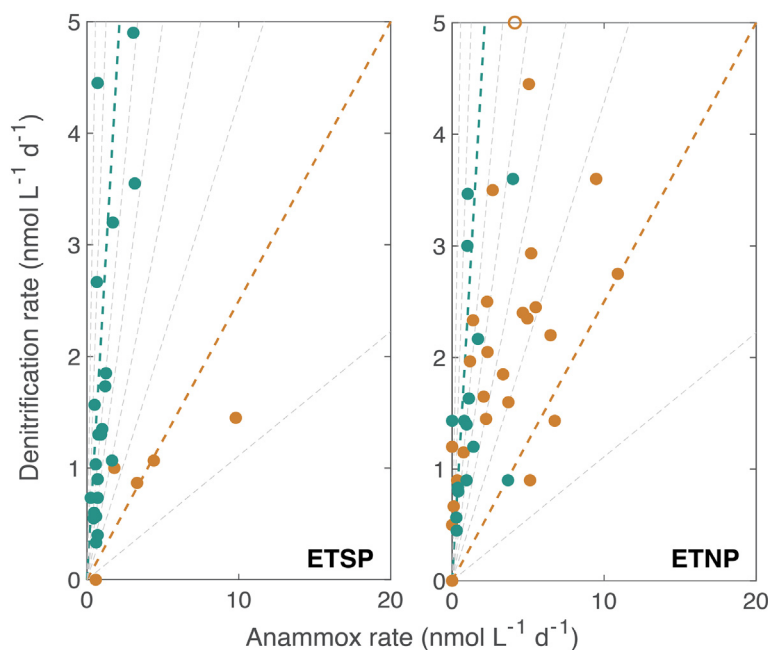
Fig. 3. Relationship between anammox and denitrification rates. The measured anammox and denitrification rates from both basins are shown, with shallow boundary samples ($\sigma_\theta < 26.4$) plotted in orange and those in the core ($\sigma_\theta > 26.4$) in teal. Contours demarking fraction of anammox, from 10% to 90% are shown. The core samples tend to be closer to ~30% anammox (teal contour), whereas the shallower samples exhibit enhanced anammox, up to ~80% (orange contour). The open circle indicates rates exceeding the shown scale but is scaled appropriately to reflect the ratio of anammox to denitrification. (For interpretation of the references to color in this figure legend, the reader is referred to the web version of this article.)
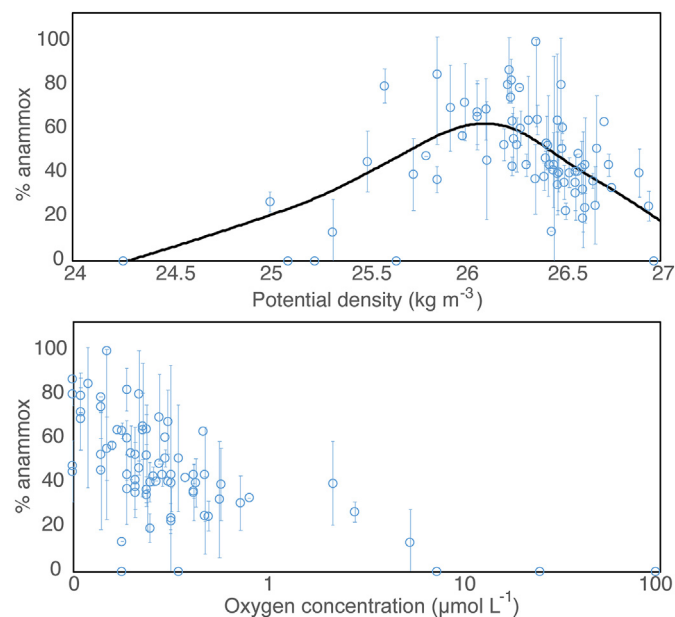

Fig. 4. Effect of depth and oxygen on fraction anammox. The proportion of fixed nitrogen loss attributed to anammox varies with respect to potential density and dissolved oxygen concentrations. Top panel: Relative amount of anammox compared to denitrification is shown as a function of potential density. A spline interpolant is shown through the data, with anammox exhibiting its largest relative rate in the shallow ODZ depths. Bottom panel: The fraction of anammox decays with increasing oxygen concentrations > 1 μmol L^{-1}, albeit with limited sampling resolution. Given the differences in Seabird SBE43 electrodes between the two ships, and the limited ability of these sensors to resolve the lowest oxygen data, the minimum oxygen measured on each cruise was substracted from all the data (1.54 and 2.09 μmol L^{-1} for the ETNP and ETSP, respectively).

in the incubations and supports that the NO_2^- oxidation rates we observe here likely result from anaerobic metabolisms. NO_2^- oxidation observed in the equatorial Pacific is thus different than that recently observed in the similar, but not quite anoxic Bay of Bengal (Bristow et al., 2017).

4.3. Observations supporting alternative pathways other than canonical aerobic NO_2^- oxidation

Whereas all known nitrite oxidizing organisms are obligate aerobes, we hypothesize alternative oxidants have a role in generating the rates observed here. This assertion derives from a methodical consideration of multiple observations from this study and from previous work, and does not exclude a role for oxygen in this process.

(1) We observed linear time courses of $^{15}NO_3^-$ production, whereas an initial acceleration or final deceleration in production would be expected if the samples were initially contaminated with O_2 and the contaminant is consumed without replenishment. This is especially true given the ~0.2–1 μmol L^{-1} half saturation coefficient for NO_2^- oxidation kinetics (Bristow et al., 2016; Sun et al., 2017). Each of the 15 time points (Fig. 2) results from a single incubation vial, arguing against random contamination during handling.

(2) Reduced NO_2^- oxidation rates in the shallowest samples (which in situ are more exposed to O_2) compared to those from the ODZ core, indicate that when O_2 was removed ex situ for incubation, aerobic nitrifiers could not function. Differential contamination of each sample from different depths is highly unlikely.

(3) O_2 contamination cannot explain the previously reported enhancement of NO_2^- oxidation by the addition of iodate (Babbin et al., 2017). Amending samples with iodate would not affect the O_2 utilization rate and thus the microbes themselves are primed to harness alternative oxidants to oxidize NO_2^-.

(4) The final helium purge prior to incubation reduces the N_2 in the vials by upwards of 99% based on mass spectrometer measurements (not shown). Assuming the same dynamics for O_2 despite the faster equilibration kinetics of O_2 compared with N_2 (Wanninkhof, 1992; Keeling et al., 1998), even a liberal contamination of 1 μmol L^{-1} of O_2 during sampling would result in less than 10 nmol L^{-1} contamination in the incubations.

(5) Recent experiments from the ETNP, amending O_2 back into purged samples from the shallowest anoxic ODZ waters, showed a marked inhibition of NO_2^- oxidation, even with a 30 nmol L^{-1} O_2 amendment (Sun et al., 2017). This inhibition suggests an alternate pathway for nitrite oxidation without oxygen.
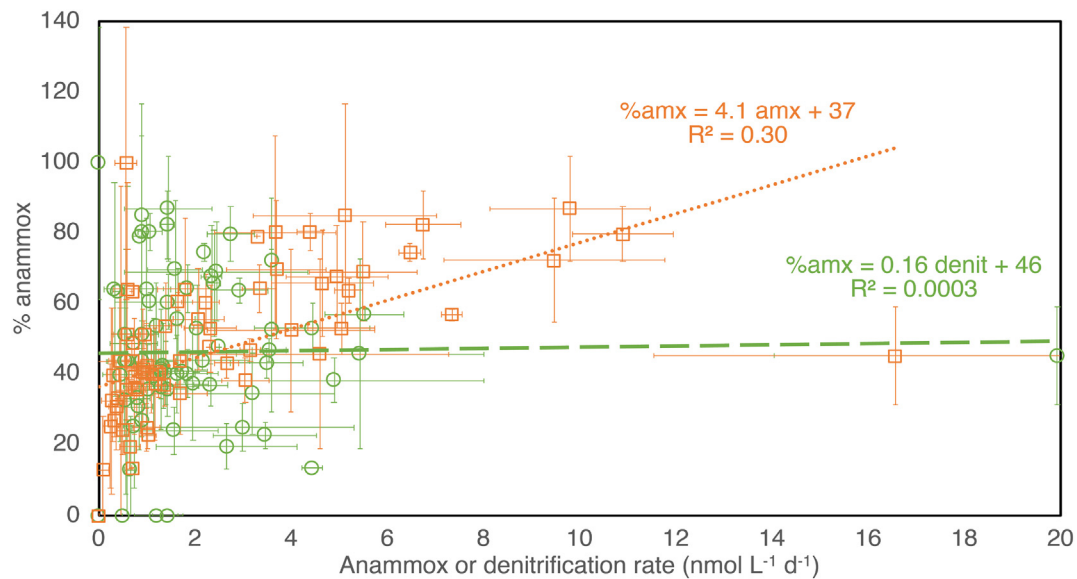
Fig. 5. Relative importance of anammox and denitrification in setting the fraction of anammox. The relative proportion of anammox is determined by the deviation in the rate of anammox much more than the rate of denitrification. Indeed, there is no statistical relationship between denitrification and the fraction of anammox despite the denitrification rate being necessary for the calculation. In other words, enhanced fraction of anammox is due to greater rates of anammox rather than lower rates of denitrification.
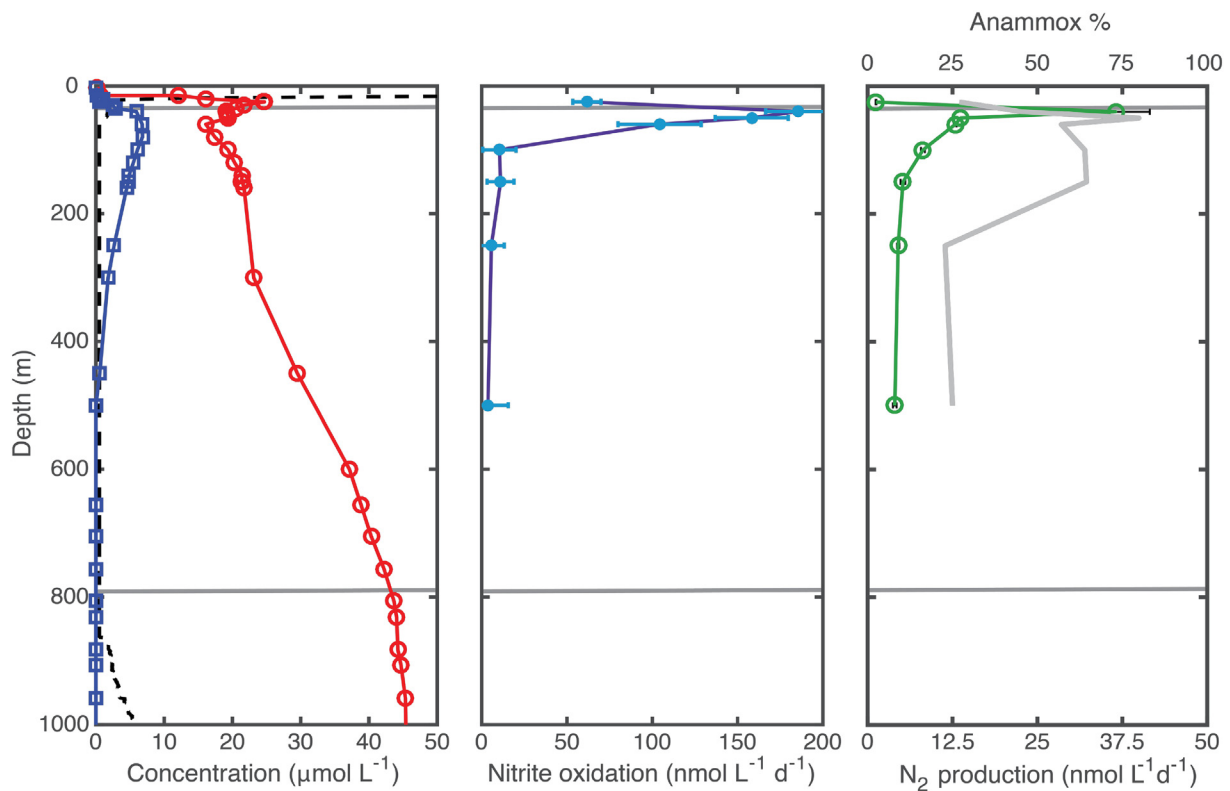

Fig. 6. Depth profiles from the ETNP coastal station. (A) Oxygen (black dashed line), nitrite (blue) and nitrate (red) concentrations are shown. (B) Nitrite oxidation rates (C) N_2 production rates (green) and the percentage of N_2 production attributed to anammox (grey). Horizontal grey lines denote suboxic/anoxic boundaries of the ODZ. (For interpretation of the references to color in this figure legend, the reader is referred to the web version of this article.)

4.4. Potential oxidants of NO_2^- under low to no oxygen

The consistent profiles at all four stations suggest that the upper oxic/anoxic boundary (and perhaps the lower one as well) represents a niche environment for microbes to oxidize NO_2^- with little to no oxygen. We can suggest several potential oxidants and mechanisms, but all require further investigation. In this zone NO_2^- is actively supplied

via NO_3^- reduction and diffusion from the core of the ODZ. As observed at the coastal ETSP site where contemporaneous NO_3^- reduction to NO_2^- experiments were conducted, NO_3^- reduction rates were generally larger, up to 120 nmol L^{-1} d^{-1}, making them fully capable of supporting all NO_2^- oxidation and reduction rates (Babbin et al., 2017). Potential oxidants at the ODZ boundaries may be supplied from the adjacent oxic water (Casciotti and Buchwald, 2012; Babbin et al., 2017). Iodate,
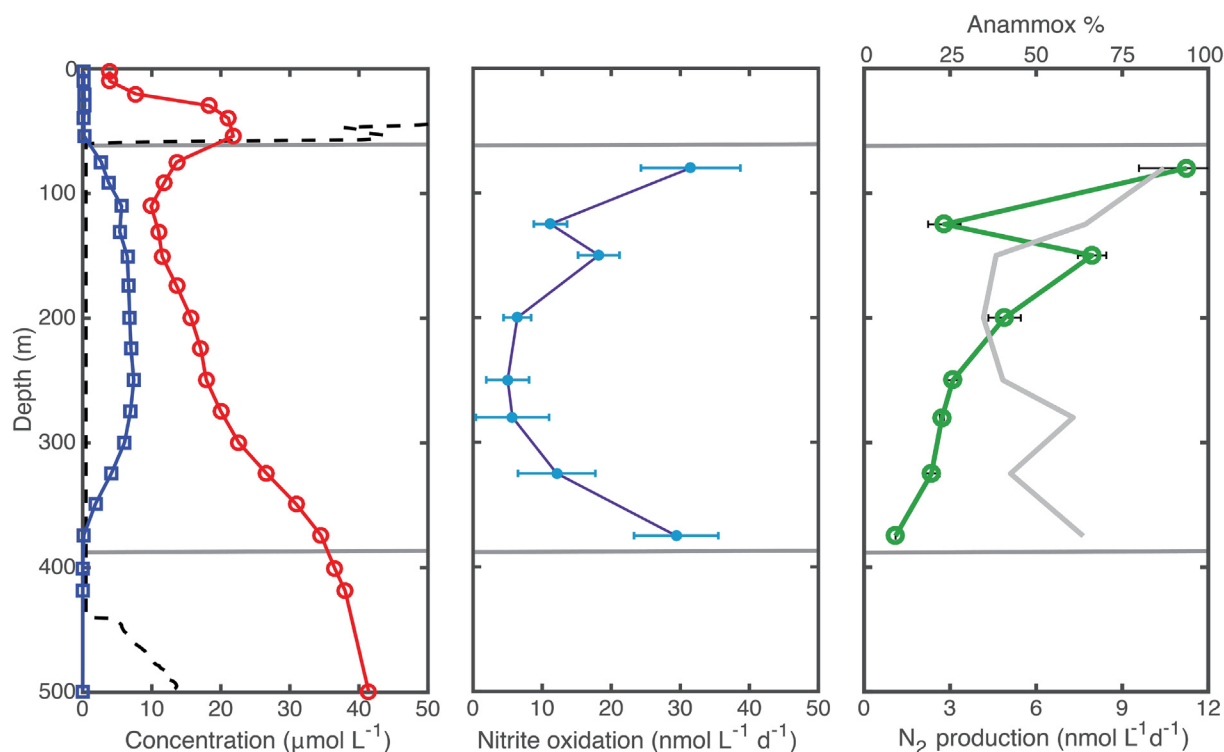
Fig. 7. Depth profiles from the ETSP coastal station. (A) Oxygen (black dashed line), nitrite (blue) and nitrate (red) concentrations are shown. (B) Nitrite oxidation rates (C) N$_2$ production rates (green) and the percentage of N$_2$ production attributed to anammox (grey). Horizontal grey lines denote suboxic/anoxic boundaries of the ODZ. (For interpretation of the references to color in this figure legend, the reader is referred to the web version of this article.)

Fig. 8. Depth profiles from the ETNP offshore station. (A) Oxygen (black dashed line), nitrite (blue) and nitrate (red) concentrations are shown. (B) Nitrite oxidation rates (C) N$_2$ production rates (green) and the percentage of N$_2$ production attributed to anammox (grey). Horizontal grey lines denote suboxic/anoxic boundaries of the ODZ. (For interpretation of the references to color in this figure legend, the reader is referred to the web version of this article.)
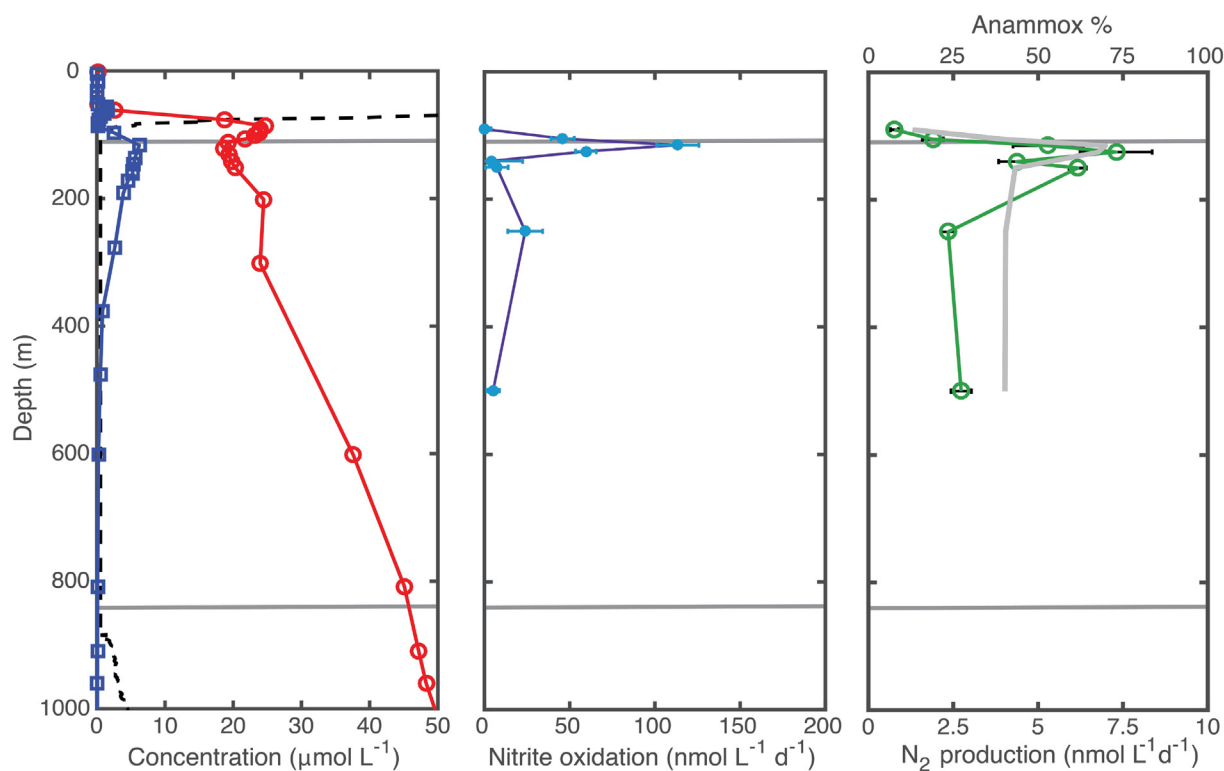
Fig. 9. Depth profiles from the ETSP offshore station. (A) Oxygen (black dashed line), nitrite (blue) and nitrate (red) concentrations are shown. (B) Nitrite oxidation rates (C) N_2 production rates (green) and the percentage of N_2 production attributed to anammox (grey). Horizontal grey lines denote suboxic/anoxic boundaries of the ODZ. (For interpretation of the references to color in this figure legend, the reader is referred to the web version of this article.)
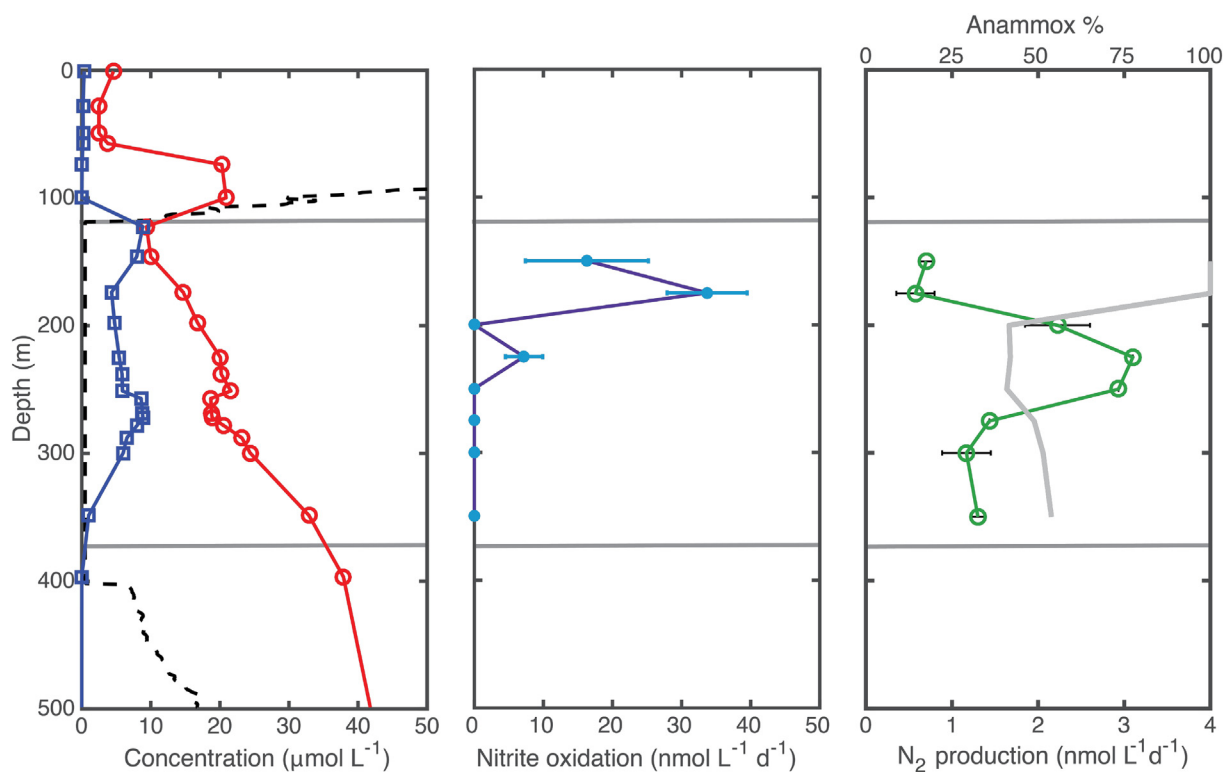
which is present at approximately 0.5 μmol L^{-1} concentrations (Nozaki, 1997; Farrenkopf and Luther, 2002) in the oxygenated ocean but disappears in the ODZ, is one likely oxidant, and each iodate reduced to iodide can oxidize up to 3 NO_2^- molecules with favorable energetics. Recent work has demonstrated the ability of iodate to stimulate NO_2^- oxidation by anaerobic ETSP communities (Babbin et al., 2017). These two fluxes, of NO_2^- and of an oxidant, collude to provide both a substrate and an oxidant for NO_2^- oxidizers. Oxygenic *Prochlorococcus* spp. could supply O_2 to support NO_2^- oxidation (Garcia-Robledo et al., 2017), but these cells are highly confined to layers with sufficient light for photosynthesis and our incubations were conducted in the dark. The rapid cycling between NO_2^- and NO_3^- may also be catalyzed by the nitrite oxidoreductase enzyme responding to low O_2 stress as suggested by a recent study in the Southern Ocean (Kemeny et al., 2016), although this reaction would be ephemeral without an active resupply of oxidative power.

Within the ODZ core, however, despite significant NO_3^- reduction supplying NO_2^-, the external oxidant supply is at a minimum, and another mechanism is necessary to explain the observed anaerobic NO_2^- oxidation rates. There are no obvious oxidants present at a high enough concentration to oxidize NO_2^- within the ODZ core (Casciotti et al., 2013) even when accounting for anammox. For the anammox metabolism, the ratio of NO_2^- oxidation to NO_2^- reduction is ~0.1, meaning the observed NO_2^- oxidation rates are in great excess of the NO_2^- oxidized in support of anammox autotrophy (Strous et al., 1998; Oshiki et al., 2016). It is possible the oxidant is NO_2^- itself. The net dismutation reaction, $2H^+ + 5NO_2^- \rightarrow N_2 + 3NO_3^- + H_2O$, is energetically favorable under in situ conditions, releasing ~60 kJ per mol of NO_2^- (Fig. 10). Our data from the core of the anoxic water exhibit an average ratio of NO_2^- oxidation/reduction of 1.5 ± 0.4 (se) ($N = 21$; Supplementary Table 1), consistent with the 1.5 expected from the proposed dismutation equation.

Such a dismutation mechanism has been proposed as one of two missing links in N cycling on the basis of discrepancies between
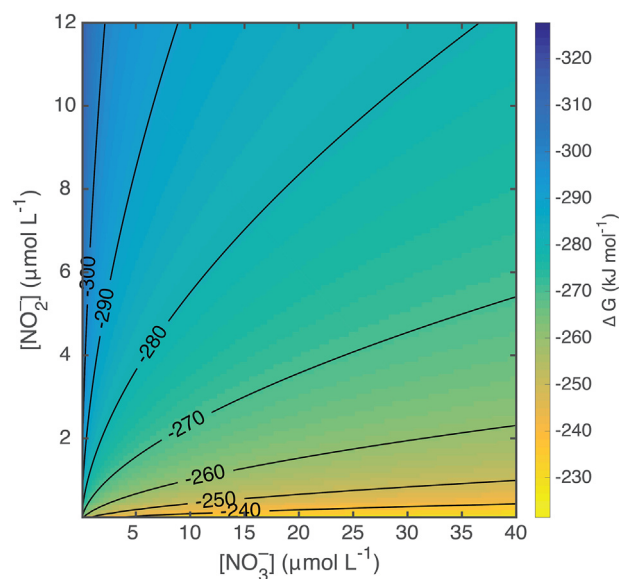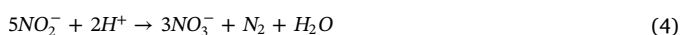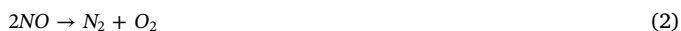

Fig. 10. Thermodynamic favorability of nitrite dismutation reaction. The calculated Gibbs free energy for the full reaction $2H^+ + 5NO_2^- \rightarrow N_2 + 3NO_3^- + H_2O$ is shown in colors and contours for a range of NO_2^- and NO_3^- concentrations in situ. Calculations are done for a N_2 concentration of 500 μmol L^{-1} and a pH of 8.

observations and first principle energetic predictions (van de Leemput et al., 2011). We hypothesize that such a dismutation mechanism may consist of three successive reaction steps that are all known to be biologically catalyzed, and two of which—NO disproportionation and NO_2^- oxidation by O_2—have been shown in the eastern tropical Pacific. Indeed, putative genes for NO disproportionation to N_2 and O_2 have been found to be transcriptionally active within the anoxic core of the

ETNP ODZ but absent above and below (Padilla et al., 2016).

The only known NO_2^- dismutase in curated protein databases is derived from the parasitic insect *Rhodnius prolixus* (He and Knipp, 2009; Knipp and He, 2011), which utilizes this pathway to create nitric oxide (NO) to dilate the red blood cells of its host (Eq. 1). Not surprisingly given the genetic dissimilarity between insects and bacteria, this gene was not found to be similar to any in the bacterial metagenome of the ETSP ODZ using BLAST tools currently available (Ganesh et al., 2014). Nevertheless, if NO were produced by NO_2^- dismutation, the NO product may in turn disproportionate into N_2 and O_2 (Eq. 2), as has been theorized (Ettwig et al., 2010). Comparing sequences from a depth-resolved ETSP metagenome (Ganesh et al., 2014) and the two putative NO dismutases in the methanotroph *Methylomirabilis oxyfera* genome, DAMO2434 and DAMO2437, (Ettwig et al., 2012) results in 13 and 16 significant hits, respectively (E-value < 10^{-10}, Score > 75) for both genes, but only from the anoxic depths and not the water above or below the ODZ core (Table 2). Significant concentrations of both gene transcripts were also reported in the ETNP, again only within the anoxic core and peaking in the center of the ODZ (Padilla et al., 2016). Finding these genes and active transcripts within the anoxic ODZ core implies some anaerobic organisms related to *M. oxyfera* can actively disproportionate NO into N_2 and O_2, although the magnitude of this rate remains to be determined. The ETNP study attempted to link this O_2 production with the oxidation of methane to remove the generated O_2, but genes for methane oxidation were not found. NO_2^-, however, is readily oxidized with O_2 to NO_3^-; and NO_2^- oxidizing bacteria and the known gene, nitrite oxidoreductase, are both abundant in ODZs (Ganesh et al., 2014; Buchwald et al., 2015; Kalvelage et al., 2015). Such intracellular O_2 generation from NO disproportionation coupled to NO_2^- oxidation (Eq. 3) complements observations from two field studies that found that very low O_2 concentrations reduce NO_2^- oxidation rates only slightly (Füssel et al., 2011; Kalvelage et al., 2013). Combined, the net reaction of these three steps (Eq. 4) is the proposed dismutation mechanism predicted on first principles (van de Leemput et al., 2011):

$$3NO_2^- + 2H^+ \rightarrow NO_3^- + 2NO + H_2O \quad (1)$$

$$2NO \rightarrow N_2 + O_2 \quad (2)$$

$$2NO_2^- + O_2 \rightarrow 2NO_3^- \quad (3)$$

$$5NO_2^- + 2H^+ \rightarrow 3NO_3^- + N_2 + H_2O \quad (4)$$
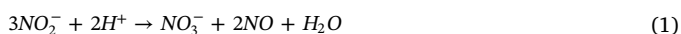
We note that a similar schematic can also be constructed via the catalytic recycling between Mn (II) and Mn (IV) (Luther, 2010; Luther et al., 1997, 2018). Dissolved manganese exists in approximately 1 nmol L^{-1} concentrations in the ETSP (Resing et al., 2015), and both the oxidization of Mn (II) by nitrate and the reduction of Mn (IV) by nitrite are energetically favorable under observed ODZ pH and chemical concentrations. The net reaction catalyzed by Mn would result in the same net dismutation reaction as Eq. 4.

5. Implications of NO_2^- oxidation in anoxic systems

More data are required to pinpoint the exact oxidants and mechanisms by which nitrite could be oxidized anaerobically in the oxygen deficient zones. Regardless of the pathway(s) by which NO_2^- oxidation occurs, however, the fact that the rates are so consistently high at the boundaries of the ODZs has implications for how fixed N is lost from the environment and therefore for marine biogeochemistry as a whole. Instead of being regions dominated by successive NO_3^- and NO_2^- reduction to N_2, ODZ boundaries apparently act as "NO_x engines" whereby NO_3^- and NO_2^- are rapidly cycled (Fig. 11). The cycling is fundamentally fueled by an organic matter energy source for NO_3^- reduction. Microbial communities utilize organic matter supplied from surface primary production to reduce NO_3^- and an oxidant mixed in from the edges to re-oxidize NO_2^- back to NO_3^-. N_2 production still

occurs within these regions of course, but much more slowly than the rapid recycling between oxidized N species. This coupled cycling results in a net release of ammonium via remineralization of organic N from sinking biomass, especially at the oxic/anoxic interface. This ammonium, which does not accumulate to measurable levels, in turn enhances the production of N_2 via anammox relative to denitrification, and explains the disparate (and unexpected) observations of anammox dominance in the Pacific ODZs (Dalsgaard et al., 2003; Hamersley et al., 2007; Lam et al., 2009; Kalvelage et al., 2013; Bianchi et al., 2014). The rate depth profiles show exactly this: NO_2^- oxidation rates and the contribution of anammox to N_2 production resemble each other closely, such that anammox exceeds 75% of total N_2 production in the same boundary regions where NO_2^- oxidation is highest (Figs. 6-9). The relative importances of anammox and denitrification in setting the fraction of anammox (Fig. 5) also point to the dominant control being nitrite oxidation rates: denitrification is not affected by nitrite oxidation and thus is not systematically changed even when anammox increases due to the greater ammonium flux. This implies that denitrification is indeed not limited by NO_2^- availability, and is consistent with more N_2O production from NO_3^- without exchange with the ambient NO_2^- pool (Ji et al., 2015).

These data corroborate the implication by natural abundance isotope studies that more than half of the nitrate reduced to nitrite in anoxic marine systems may be regenerated by nitrite re-oxidation rather than reduced fully to N_2 gas (Granger and Wankel, 2016). This nitrite is well in excess of what anammox can supply stoichiometrically. Natural abundance studies also imply denitrification and nitrite oxidation co-occur in the environment, which we have directly demonstrated with simultaneous measurements of NO_2^- reduction to N_2 and oxidation to NO_3^- in the same incubation vials (Buchwald et al., 2015; Granger and Wankel, 2016; Peters et al., 2016).

Fast anaerobic N cycling between bioavailable forms compared to N_2 production has implications for global primary productivity and ocean fertility (Ward, 2013), especially if the volume of ODZs changes into the future (Stramma et al., 2008; Codispoti, 2010; Deutsch et al., 2014). Significant NO_2^- oxidation shifts our view of the dominant metabolisms in the ODZs from a loss of fixed N to a cycling between bioavailable forms. Biogeochemical models currently require parameterization that artificially lowers respiration rates in ODZs in order to prevent complete NO_3^- consumption (Su et al., 2015). With the rapid recycling mechanism between NO_3^- and NO_2^- shown by our data, high remineralization rates in ODZs are permitted without complete NO_3^- drawdown.

A perhaps wider-reaching implication of decoupling denitrification between the NO_3^- and NO_2^- reduction steps and NO_2^- re-oxidation returning NO_2^- to NO_3^- is with respect to the calculation of the global marine N budget. The global marine N loss budget is calculated through combination of geochemical measurements of both concentrations and isotopes, and relies on a number of assumptions. Water column denitrification is calculated from a deficit in fixed N relative to phosphorus and from direct measurements of rates (Codispoti et al., 2001; Deutsch et al., 2001; Ward et al., 2009; Chang et al., 2010, 2012). Sedimentary denitrification, however, must be inferred using isotope balance with known fractionation factors because of the heterogeneity of sedimentary processes across the global seafloor (Brandes and Devol, 2002; Sigman et al., 2009). Significant NO_2^- oxidation in the ODZ water column would alter the modern marine N budget calculation. Some estimates suggest that the oceans would be fully devoid of fixed N within a few thousand years due to excess denitrification over N_2 fixation (Codispoti, 2007), but such budgets rely heavily on choosing a fractionation factor for denitrification to balance observed natural abundance isotopes (Brandes and Devol, 2002). Because NO_2^- oxidation occurs with a large inverse isotope effect (Casciotti, 2009) and critically, the contribution of anaerobic NO_2^- oxidation to overall N cycling varies substantially with depth, a single choice of ODZ fractionation factor based on water column data may not be appropriate. Treating the
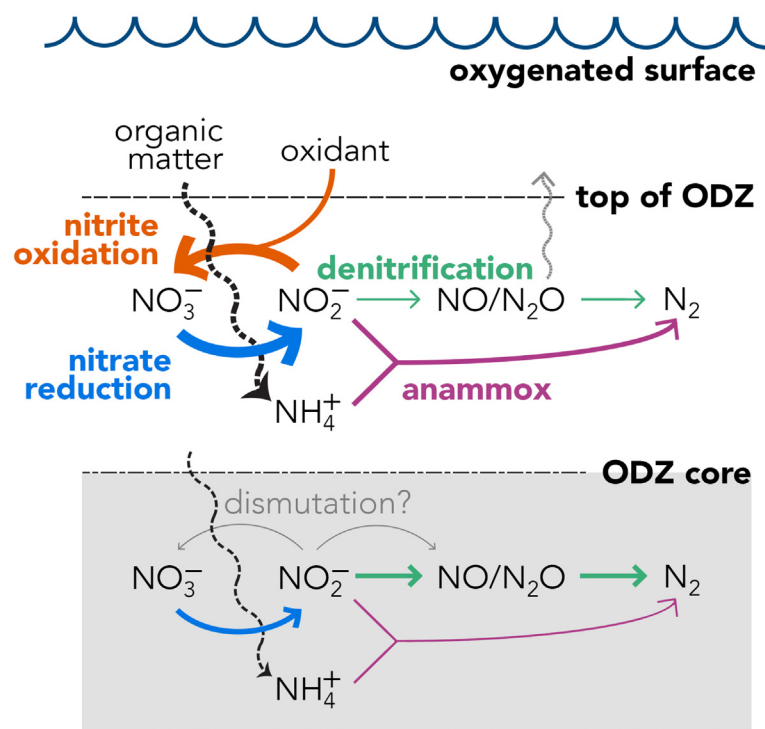
Fig. 11. Schematic of anaerobic nitrogen cycle. The microbial N transformations for the top and core of the ODZ are shown, split into two distinct regions based on oxidant supply. Organic matter sinking from the overlying water drives the biogeochemistry. The significant difference between the two regimes is that in the top, where an external oxidant is supplied from the oxygenated surface, the NO_3^-/NO_2^- cycle is rapid compared to further NO_2^- reduction. This catalyzes organic matter respiration and releases ammonium to enhance anammox over denitrification. In the core, however, NO_2^- oxidation via possible dismutation is slower, with only a small effect on the anammox / denitrification ratio. The arrow thicknesses are qualitative, indicating that in the upper ODZ, nitrite oxidation and nitrate reduction far exceed rates of anammox and denitrification.

ODZ as a single box can obscure the true isotopic balance imparted by a complex and variable set of metabolisms. Data from some culture studies would lower the fractionation factor for denitrification (Kritee et al., 2012), which would in turn reduce the globally calculated denitrification rate. NO_2^- oxidation, especially at the boundaries, increases the heavy isotopic composition of NO_3^- and could allow reconciliation of culture data with environmental samples by increasing the net observed fractionation factor.

NO_2^- oxidation in the environment, both in the ODZs and other anoxic systems, merits further exploration, but our data provide a starting point for such studies to investigate what factors control what transformations and which microorganisms are involved. The exact distribution and mechanisms of nitrite oxidation in ODZs remains to be fully elucidated. The relative roles of the multiple oxidizing compounds, i.e, O_2, IO_3^-, NO_2^- (dismutation), and Mn^{4+} (via catalytic recycling) remain to be explored through a series of directed experiments with depth and across the regions. Moreover the organisms responsible for these transformations must be isolated and cultured to gain a clear understanding of the specific mechanistic steps. Such research avenues, across the multiple ODZs, will provide the necessary data to explain the paradox of rates of nitrite oxidation exceeding reduction under anoxic conditions. Substantive NO_2^- oxidation not only acts to further complicate the known N cycling reactions in ODZs, but also changes our understanding of the dominant metabolisms in these dynamic regions and how the microbial community interacts to control geochemistry.

Author contributions

A.R.B. and B.B.W. designed and conducted the onboard incubations, and A.R.B., C.B., and S.D.W. performed the mass spectrometry analysis. A.R.B., F.M.M.M., and B.B.W. wrote the paper with contribution from all authors. All data presented in this paper are available in the Supplementary Materials.

Acknowledgements

Appendix A. Supplementary data

Supplementary data to this article can be found online at https://doi.org/10.1016/j.marchem.2020.103814.

References

Babbin, A.R., Keil, R.G., Devol, A.H., Ward, B.B., 2014. Organic matter stoichiometry, flux, and oxygen control nitrogen loss in the ocean. Science 344, 406–408. https://doi.org/10.1126/science.1248364.

Babbin, A.R., Bianchi, D., Jayakumar, A., Ward, B.B., 2015. Rapid nitrous oxide cycling in the suboxic ocean. Science 348, 1127–1129. https://doi.org/10.1126/science.aaa8380.

Babbin, A.R., Peters, B.D., Mordy, C.W., Widner, B., Casciotti, K.L., Ward, B.B., 2017. Multiple metabolisms constrain the anaerobic nitrite budget in the Eastern Tropical South Pacific. Glob. Biogeochem. Cycles 31. https://doi.org/10.1002/2016GB005407.

Beman, J.M., Leilei Shih, J., Popp, B.N., 2013. Nitrite oxidation in the upper water column and oxygen minimum zone of the eastern tropical North Pacific Ocean. ISME J. 7, 2192–2205. https://doi.org/10.1038/ismej.2013.96.

Betlach, M.R., Tiedje, J.M., 1981. Kinetic explanation for accumulation of nitrite, nitric oxide, and nitrous oxide during bacterial denitrification. Appl. Environ. Microbiol. 42, 1074–1084.

Bianchi, D., Babbin, A.R., Galbraith, E.D., 2014. Enhancement of anammox by the excretion of diel vertical migrators. Proc. Natl. Acad. Sci. 111, 15653–15658. https://doi.org/10.1073/pnas.1410790111.

Bianchi, D., Weber, T.S., Kiko, R., Deutsch, C., 2018. Global niche of marine anaerobic metabolisms expanded by particle microenvironments. Nat. Geosci. 11, 263–268. https://doi.org/10.1038/s41561-018-0081-0.

Brandes, J.A., Devol, A.H., 2002. A global marine-fixed nitrogen isotopic budget: Implications for Holocene nitrogen cycling. Glob. Biogeochem. Cycles 16, 1120. https://doi.org/10.1029/2001GB001856.

Bristow, L.A., Dalsgaard, T., Tiano, L., Mills, D.B., Bertagnolli, A.D., Wright, J.J., Hallam, S.J., Ulloa, O., Canfield, D.E., Revsbech, N.P., Thamdrup, B., 2016. Ammonium and nitrite oxidation at nanomolar oxygen concentrations in oxygen minimum zone waters. Proc. Natl. Acad. Sci. U. S. A. 113, 10601–10606. https://doi.org/10.1073/pnas.1600359113.

Bristow, L.A., Callbeck, C.M., Larsen, M., Altabet, M.A., Dekaezemacker, J., Forth, M., Gauns, M., Glud, R.N., Kuypers, M.M.M., Lavik, G., Milucka, J., Naqvi, S.W.A.,

Partihary, A., Revsbech, N.P., Thamdrup, B., Treusch, A.H., Canfield, D.E., 2017. N_2 production rates limited by nitrite availability in the Bay of Bengal oxygen minimum zone. Nat. Geosci. 10, 24–29. https://doi.org/10.1038/ngeo2847.

Brunner, B., Contreras, S., Lehmann, M.F., Matantseva, O., Rollog, M., Kalvelage, T., Klockgether, G., Lavik, G., Jetten, M.S.M., Kartal, B., Kuypers, M.M.M., 2013. Nitrogen isotope effects induced by anammox bacteria. Proc. Natl. Acad. Sci. 110, 18994–18999. https://doi.org/10.1073/pnas.1310488110.

Buchwald, C., Santoro, A.E., Stanley, R.H.R., Casciotti, K.L., 2015. Nitrogen cycling in the secondary nitrite maximum of the Eastern Tropical North Pacific off Costa Rica. Glob. Biogeochem. Cycles 29, 2061–2081. https://doi.org/10.1002/2015GB005187.

Bulow, S.E., Rich, J.J., Naik, H.S., Pratihary, A.K., Ward, B.B., 2010. Denitrification exceeds anammox as a nitrogen loss pathway in the Arabian Sea oxygen minimum zone. Deep. Res. I 57, 384–393. https://doi.org/10.1016/j.dsr.2009.10.014.

Casciotti, K.L., 2009. Inverse kinetic isotope fractionation during bacterial nitrite oxidation. Geochim. Cosmochim. Acta 73, 2061–2076. https://doi.org/10.1016/j.gca.2008.12.022.

Casciotti, K.L., Buchwald, C., 2012. Insights on the marine microbial nitrogen cycle from isotopic approaches to nitrification. Front. Microbiol. 3. https://doi.org/10.3389/fmicb.2012.00356.

Casciotti, K.L., Buchwald, C., McIlvin, M., 2013. Implications of nitrate and nitrite isotopic measurements for the mechanisms of nitrogen cycling in the Peru oxygen deficient zone. Deep. Res. I 80, 78–93. https://doi.org/10.1016/j.dsr.2013.05.017.

Chang, B.X., Devol, A.H., Emerson, S.R., 2010. Denitrification and the nitrogen gas excess in the eastern tropical South Pacific oxygen deficient zone. Deep. Res. I 57, 1092–1101. https://doi.org/10.1016/j.dsr.2010.05.009.

Chang, B.X., Devol, A.H., Emerson, S.R., 2012. Fixed nitrogen loss from the eastern tropical North Pacific and Arabian Sea oxygen deficient zones determined from measurements of N_2:Ar. Glob. Biogeochem. Cycles 26, GB3030. https://doi.org/10.1029/2011GB004207.

Codispoti, L.A., 2007. An oceanic fixed nitrogen sink exceeding 400 Tg N a^{-1} vs the concept of homeostasis in the fixed-nitrogen inventory. Biogeosciences 4, 233–253.

Codispoti, L.A., 2010. Interesting times for marine N_2O. Science 327, 1339–1340. https://doi.org/10.1126/science.1184945.

Codispoti, L.A., Brandes, J.A., Christensen, J.P., Devol, A.H., Naqvi, S.W.A., Paerl, H.W., Yoshinari, T., 2001. The oceanic fixed nitrogen and nitrous oxide budgets: moving targets as we enter the anthropocene? Sci. Mar. 65, 85–105.

Dalsgaard, T., Canfield, D.E., Petersen, J., Thamdrup, B., Acuña-González, J., 2003. N_2 production by the anammox reaction in the anoxic water column of Golfo Dulce, Costa Rica. Nature 422, 606–608. https://doi.org/10.1038/nature01526.

Dalsgaard, T., Thamdrup, B., Farías, L., Revsbech, N.P., 2012. Anammox and denitrification in the oxygen minimum zone of the eastern South Pacific. Limnol. Oceanogr. 57, 1331–1346. https://doi.org/10.4319/lo.2012.57.5.1331.

Dalsgaard, T., Stewart, F.J., Thamdrup, B., De Brabandere, L., Revsbech, N.P., Ulloa, O., Canfield, D.E., DeLong, E.F., 2014. Oxygen at nanomolar levels reversibly suppresses process rates and gene expression in anammox and denitrification in the oxygen minimum zone off northern Chile. MBio 5, e01966. https://doi.org/10.1128/mBio.01966-14.

De Brabandere, L., Canfield, D.E., Dalsgaard, T., Friederich, G.E., Revsbech, N.P., Ulloa, O., Thamdrup, B., 2014. Vertical partitioning of nitrogen-loss processes across the oxic-anoxic interface of an oceanic oxygen minimum zone. Environ. Microbiol. 16, 1–14. https://doi.org/10.1111/1462-2920.12255.

Deutsch, C., Gruber, N., Key, R.M., Sarmiento, J.L., Ganachaud, A., 2001. Denitrification and N_2 fixation in the Pacific Ocean. Glob. Biogeochem. Cycles 15, 483–506.

Deutsch, C., Berelson, W., Thunell, R., Weber, T., Tems, C., McManus, J., Crusius, J., Ito, T., Baumgartner, T., Ferreira, V., Mey, J., van Geen, A., 2014. Centennial changes in North Pacific anoxia linked to tropical trade winds. Science 345, 665–668. https://doi.org/10.1126/science.1252332.

DiSpirito, A.A., Hooper, A.B., 1986. Oxygen exchange between nitrate molecules during nitrite oxidation by Nitrobacter. J. Biol. Chem. 261 (23), 10534–10537.

Ettwig, K.F., Butler, M.K., Le Paslier, D., Pelletier, E., Mangenot, S., Kuypers, M.M.M., Schreiber, F., Dutilh, B.E., Zedelius, J., de Beer, D., Gloerich, J., Wessels, H.J.C.T., van Alen, T., Luesken, F., Wu, M.L., van de Pas-Schoonen, K.T., Op den Camp, H.J.M., Janssen-Megens, E.M., Francoijs, K.-J., Stunnenberg, H., Weissenbach, J., Jetten, M.S.M., Strous, M., 2010. Nitrite-driven anaerobic methane oxidation by oxygenic bacteria. Nature 464, 543–548. https://doi.org/10.1038/nature08883.

Ettwig, K.F., Speth, D.R., Reimann, J., Wu, M.L., Jetten, M.S.M., Keltjens, J.T., 2012. Bacterial oxygen production in the dark. Front. Microbiol. 3, 273. https://doi.org/10.3389/fmicb.2012.00273.

Farrenkopf, A.M., Luther, G.W., 2002. Iodine chemistry reflects productivity and denitrification in the Arabian Sea: evidence for flux of dissolved species from sediments of western India into the OMZ. Deep Sea Res. Part II Top. Stud. Oceanogr. 49, 2303–2318. https://doi.org/10.1016/S0967-0645(02)00038-3.

Füssel, J., Lam, P., Lavik, G., Jensen, M.M., Holtappels, M., Günter, M., Kuypers, M.M.M., 2011. Nitrite oxidation in the Namibian oxygen minimum zone. ISME J. 6, 1200–1209. https://doi.org/10.1038/ismej.2011.178.

Ganesh, S., Parris, D.J., DeLong, E.F., Stewart, F.J., 2014. Metagenomic analysis of size-fractionated picoplankton in a marine oxygen minimum zone. ISME J 8, 187–211. https://doi.org/10.1038/ismej.2013.144.

Garcia, H.E., Weathers, K., Paver, C.R., Smolyar, I., Boyer, T.P., Locarnin, R.A., Zweng, M.M., Mishonov, A.V., Baranova, O.K., Seidov, D., Reagan, J.R., 2018. World Ocean Atlas 2018, Volume 3: Dissolved oxygen, apparent oxygen utilization, and oxygen saturation. In: Mishonov, A. (Ed.), NOAA Atlas NESDIS 83.

Garcia-Robledo, E., Padilla, C.C., Aldunate, M., Stewart, F.J., Ulloa, O., Paulmier, A., Gregori, G., Revsbech, N.P., 2017. Cryptic oxygen cycling in anoxic marine zones. Proc. Natl. Acad. Sci. 114 (31), 8319–8324. https://doi.org/10.1073/pnas.1619844114.

Granger, J., Sigman, D.M., 2009. Removal of nitrite with sulfamic acid for nitrate N and O isotope analysis with the denitrifier method. Rapid Commun. Mass Spectrom. 23, 3753–3762. https://doi.org/10.1002/rcm.4307.

Granger, J., Wankel, S.D., 2016. Isotopic overprinting of nitrification on denitrification as a ubiquitous and unifying feature of environmental nitrogen cycling. Proc. Natl. Acad. Sci. 113 (42), E6391–E6400. https://doi.org/10.1073/pnas.1601383113.

Hamersley, M.R., Lavik, G., Woebken, D., Rattray, J.E., Lam, P., Hopmans, E.C., Damsté, J.S.S., Krüger, S., Graco, M., Gutiérrez, D., Kuypers, M.M.M., 2007. Anaerobic ammonium oxidation in the Peruvian oxygen minimum zone. Limnol. Oceanogr. 52, 923–933.

He, C., Knipp, M., 2009. Formation of Nitric Oxide from Nitrite by the Ferriheme bProtein Nitrophorin 7. J. Am. Chem. Soc. 131, 12042–12043. https://doi.org/10.1021/ja9040362.

Ji, Q., Babbin, A.R., Jayakumar, A., Oleynik, S., Ward, B.B., 2015. Nitrous oxide production by nitrification and denitrification in the Eastern Tropical South Pacific oxygen minimum zone. Geophys. Res. Lett. 42, 10,755–10,764. https://doi.org/10.1002/2015GL066853.

Kalvelage, T., Lavik, G., Lam, P., Contreras, S., Arteaga, L., Löscher, C.R., Oschlies, A., Paulmier, A., Stramma, L., Kuypers, M.M.M., 2013. Nitrogen cycling driven by organic matter export in the South Pacific oxygen minimum zone. Nat. Geosci. 6, 228–234. https://doi.org/10.1038/ngeo1739.

Kalvelage, T., Lavik, G., Jensen, M.M., Revsbech, N.P., Löscher, C., Schunck, H., Desai, D.K., Hauss, H., Kiko, R., Holtappels, M., LaRoche, J., Schmitz, R.A., Graco, M.I., Kuypers, M.M.M., 2015. Aerobic microbial respiration in oceanic oxygen minimum zones. PLoS One 10, e0133526. https://doi.org/10.1371/journal.pone.0133526.

Keeling, R.F, Stephens, B.B Najjar, R.G., Doney, S.C., Archer, D., 1998. Seasonal variations in the atmospheric O_2/N_2 ratio in relation to the kinetics of air-sea gas exchange. Global Biogeochem. Cycles 12, 141–163. https://doi.org/10.1029/97GB02339.

Kemeny, P.C., Weigand, M.A., Zhang, R., Carter, B.R., Karsh, K.L., Fawcett, S.E., Sigman, D.M., 2016. Enzyme-level interconversion of nitrate and nitrite in the fall mixed layer of the Antarctic Ocean. Glob. Biogeochem. Cycles. https://doi.org/10.1002/2015GB005350.

Knipp, M., He, C., 2011. Nitrophorins: nitrite disproportionation reaction and other novel functionalities of insect heme-based nitric oxide transport proteins. IUBMB Life 63, 304–312. https://doi.org/10.1002/iub.451.

Kritee, K., Sigman, D.M., Granger, J., Ward, B.B., Jayakumar, A., Deutsch, C., 2012. Reduced isotope fractionation by denitrification under conditions relevant to the ocean. Geochim. Cosmochim. Acta 92, 243–259. https://doi.org/10.1016/j.gca.2012.05.020.

Lam, P., Lavik, G., Jensen, M.M., van de Vossenberg, J., Schmid, M., Woebken, D., Gutiérrez, D., Amann, R., Jetten, M.S.M., Kuypers, M.M.M., 2009. Revising the nitrogen cycle in the Peruvian oxygen minimum zone. Proc. Natl. Acad. Sci. 106, 4752–4757. https://doi.org/10.1073/pnas.0812444106.

Lam, P., Jensen, M.M., Kock, A., Lettmann, K.A., Plancherel, Y., Lavik, G., Bange, H.W., Kuypers, M.M.M., 2011. Origin and fate of the secondary nitrite maximum in the Arabian Sea. Biogeosciences 8, 1565–1577. https://doi.org/10.5194/bg-8-1565-2011.

Lees, H., Simpson, J.R., 1957. The biochemistry of the nitrifying organisms. V. Nitrite oxidation by Nitrobacter. Biochem. J. 65, 297–305.

Lipschultz, F., Wofsy, S.C., Ward, B.B., Codispoti, L.A., Friedrich, G., Elkins, J.W., 1990. Bacterial transformations of inorganic nitrogen in the oxygen-deficient waters of the eastern tropical South Pacific Ocean. Deep. Res. 37, 1513–1541.

Luther, G.W., 2010. The role of one- and two-electron transfer reactions in forming thermodynamically unstable intermediates as barriers in multi-electron redox reactions. Aquat. Geochem. 16, 395–420. https://doi.org/10.1007/s10498-009-9082-3.

Luther, G.W., Sundby, B., Lewis, B.L., Brendel, P.J., Silverberg, N., 1997. Interactions of manganese with the nitrogen cycle: Alternative pathways to dinitrogen. Geochim. Cosmochim. Acta 61, 4043–4052. https://doi.org/10.1016/S0016-7037(97)00239-1.

Luther, G.W., Thibault de Chanvalon, A., Oldham, V.E., Estes, E.R., Tebo, B.M., Madison, A.S., 2018. reduction of manganese oxides: thermodynamic, kinetic and mechanistic considerations for one- versus two-electron transfer steps. Aquat. Geochem. 24, 257–277. https://doi.org/10.1007/s10498-018-9342-1.

Martens-Habbena, W., Berube, P.M., Urakawa, H., de la Torre, J.R., Stahl, D.A., 2009. Ammonia oxidation kinetics determine niche separation of nitrifying Archaea and Bacteria. Nature 461, 976–979. https://doi.org/10.1038/nature08465.

Nozaki, Y., 1997. A fresh look at element distribution in the North Pacific Ocean. EOS Trans. Am. Geophys. Union 78, 221–223. https://doi.org/10.1029/97EO00148.

Oshiki, M., Satoh, H., Okabe, S., 2016. Ecology and physiology of anaerobic ammonium oxidizing bacteria. Environ. Microbiol. 18, 2784–2796. https://doi.org/10.1111/1462-2920.13134.

Padilla, C.C., Bristow, L.A., Sarode, N., Garcia-Robledo, E., Gómez Ramírez, E., Benson, C.R., Bourbonnais, A., Altabet, M.A., Girguis, P.R., Thamdrup, B., Stewart, F.J., 2016. NC10 bacteria in marine oxygen minimum zones. ISME J. https://doi.org/10.1038/ismej.2015.262.

Peng, X., Fuchsman, C.A., Jayakumar, A., Oleynik, S., Martens-Habbena, W., Devol, A.H., Ward, B.B., 2015. Ammonia and nitrite oxidation in the Eastern Tropical North Pacific. Glob. Biogeochem. Cycles 29, 2034–2049. https://doi.org/10.1002/2015GB005278.

Peng, X., Fuchsman, C.A., Jayakumar, A., Warner, M.J., Devol, A.H., Ward, B.B., 2016. Revisiting nitrification in the eastern tropical South Pacific: A focus on controls. J. Geophys. Res. Ocean. 1667–1684. https://doi.org/10.1002/2015JC011455.

Peters, B.D., Babbin, A.R., Lettman, K.A., Mordy, C.W., Ulloa, O., Ward, B.B., Casciotti, K.L., 2016. Vertical modeling of the nitrogen cycle in the eastern tropical south Pacific oxygen deficient zone using high resolution concentration and isotope

measurements. Glob. Biogeochem. Cycles 30, 1661–1681. https://doi.org/10.1002/2016GB005415.

Resing, J.A., Sedwick, P.N., German, C.R., Jenkins, W.J., Moffett, J.W., Sohst, B.M., Tagliabue, A., 2015. Basin-scale transport of hydrothermal dissolved metals across the South Pacific Ocean. Nature 523, 200–203. https://doi.org/10.1038/nature14577.

Revsbech, N.P., Larsen, L.H., Gundersen, J., Dalsgaard, T., Ulloa, O., Thamdrup, B., 2009. Determination of ultra-low oxygen concentrations in oxygen minimum zones by the STOX sensor. Limnol. Oceanogr. Methods 7, 371–381.

Sigman, D.M., Casciotti, K.L., Andreani, M., Barford, C., Galanter, M., Böhlke, J.K., 2001. A Bacterial Method for the Nitrogen Isotopic Analysis of Nitrate in Seawater and Freshwater. Anal. Chem. 73, 4145–4153. https://doi.org/10.1021/ac010088e.

Sigman, D.M., Granger, J., DiFiore, P.J., Lehmann, M.M., Ho, R., Cane, G., van Geen, A., 2005. Coupled nitrogen and oxygen isotope measurements of nitrate along the eastern North Pacific margin. Glob. Biogeochem. Cycles 19. https://doi.org/10.1029/2005GB002458.

Sigman, D.M., DiFiore, P.J., Hain, M.P., Deutsch, C., Wang, Y., Karl, D.M., Knapp, A.N., Lehmann, M.F., Pantoja, S., 2009. The dual isotopes of deep nitrate as a constraint on the cycle and budget of oceanic fixed nitrogen. Deep. Res. I 56, 1419–1439. https://doi.org/10.1016/j.dsr.2009.04.007.

Stramma, L., Johnson, G.C., Sprintall, J., Mohrholz, V., 2008. Expanding oxygen-minimum zones in the tropical oceans. Science 320, 655–658. https://doi.org/10.1126/science.1153847.

Strous, M., Heijnen, J.J., Kuenen, J.G., Jetten, M.S.M., 1998. The sequencing batch reactor as a powerful tool for the study of slowly growing anaerobic ammonium-oxidizing microorganisms. Appl. Microbiol. Biotechnol. 50, 589–596.

Su, B., Pahlow, M., Wagner, H., Oschlies, A., 2015. What prevents nitrogen depletion in the oxygen minimum zone of the eastern tropical South Pacific? Biogeosciences 12, 1113–1130. https://doi.org/10.5194/bg-12-1113-2015.

Sun, X., Ji, Q., Jayakumar, A., Ward, B.B., 2017. Dependence of nitrite oxidation on nitrite and oxygen in low-oxygen seawater. Geophys. Res. Lett. 44, 7883–7891. https://doi.org/10.1002/2017GL074355.

Thamdrup, B., Dalsgaard, T., 2002. Production of N_2 through anaerobic ammonium oxidation coupled to nitrate reduction in marine sediments. Appl. Environ. Microbiol. 68, 1312–1318. https://doi.org/10.1128/AEM.68.3.1312-1318.2002.

Tiano, L., Garcia-Robledo, E., Dalsgaard, T., Devol, A.H., Ward, B.B., Ulloa, O., Canfield, D.E., Peter Revsbech, N., 2014. Oxygen distribution and aerobic respiration in the north and south eastern tropical Pacific oxygen minimum zones. Deep Sea Res. Part I Oceanogr. Res. Pap. 94, 173–183. https://doi.org/10.1016/j.dsr.2014.10.001.

Tsementzi, D., Wu, J., Deutsch, S., Nath, S., Rodriguez-R, L.M., Burns, A.S., Ranjan, P., Sarode, N., Malmstrom, R.R., Padilla, C.C., Stone, B.K., Bristow, L.A., Larsen, M., Glass, J.B., Thamdrup, B., Woyke, T., Konstantinidis, K.T., Stewart, F.J., 2016. SAR11 bacteria linked to ocean anoxia and nitrogen loss. Nature. https://doi.org/10.1038/nature19068.

van de Leemput, I.A., Veraart, A.J., Dakos, V., de Klein, J.J.M., Strous, M., Scheffer, M., 2011. Predicting microbial nitrogen pathways from basic principles. Environ. Microbiol. 13, 1477–1487. https://doi.org/10.1111/j.1462-2920.2011.02450.x.

Wanninkhof, R., 1992. Relationship between wind speed and gas exchange over the ocean. J. Geophy. Res. Ocean. 97, 7373–7382. https://doi.org/10.1029/92JC00188.

Ward, B.B., 2013. How nitrogen is lost. Science 341, 352–353. https://doi.org/10.1126/science.1240314.

Ward, B.B., Devol, A.H., Rich, J.J., Chang, B.X., Bulow, S.E., Naik, H., Pratihary, A., Jayakumar, A., 2009. Denitrification as the dominant nitrogen loss process in the Arabian Sea. Nature 461, 78–81. https://doi.org/10.1038/nature08276.

Ward, B.B., Zafirou, O.C., 1988. Nitrification and nitric oxide in the oxygen minimum of the eastern tropical North Pacific. Deep Sea Res. Part A Oceanogr. Res. Pap. 35, 1127–1142. https://doi.org/10.1016/0198-0149(88)90005-2.

Nitrite oxidation exceeds reduction and fixed nitrogen loss in anoxic Pacific waters

Andrew R. Babbin[1]*, Carolyn Buchwald[2,3], François M. M. Morel[4], Scott D. Wankel[2], Bess B. Ward[4]

[1]Department of Earth, Atmospheric, and Planetary Sciences, Massachusetts Institute of Technology, Cambridge, Massachusetts 02139, USA
[2]Department of Marine Chemistry and Geochemistry, Woods Hole Oceanographic Institution, Woods Hole, Massachusetts 02543, USA
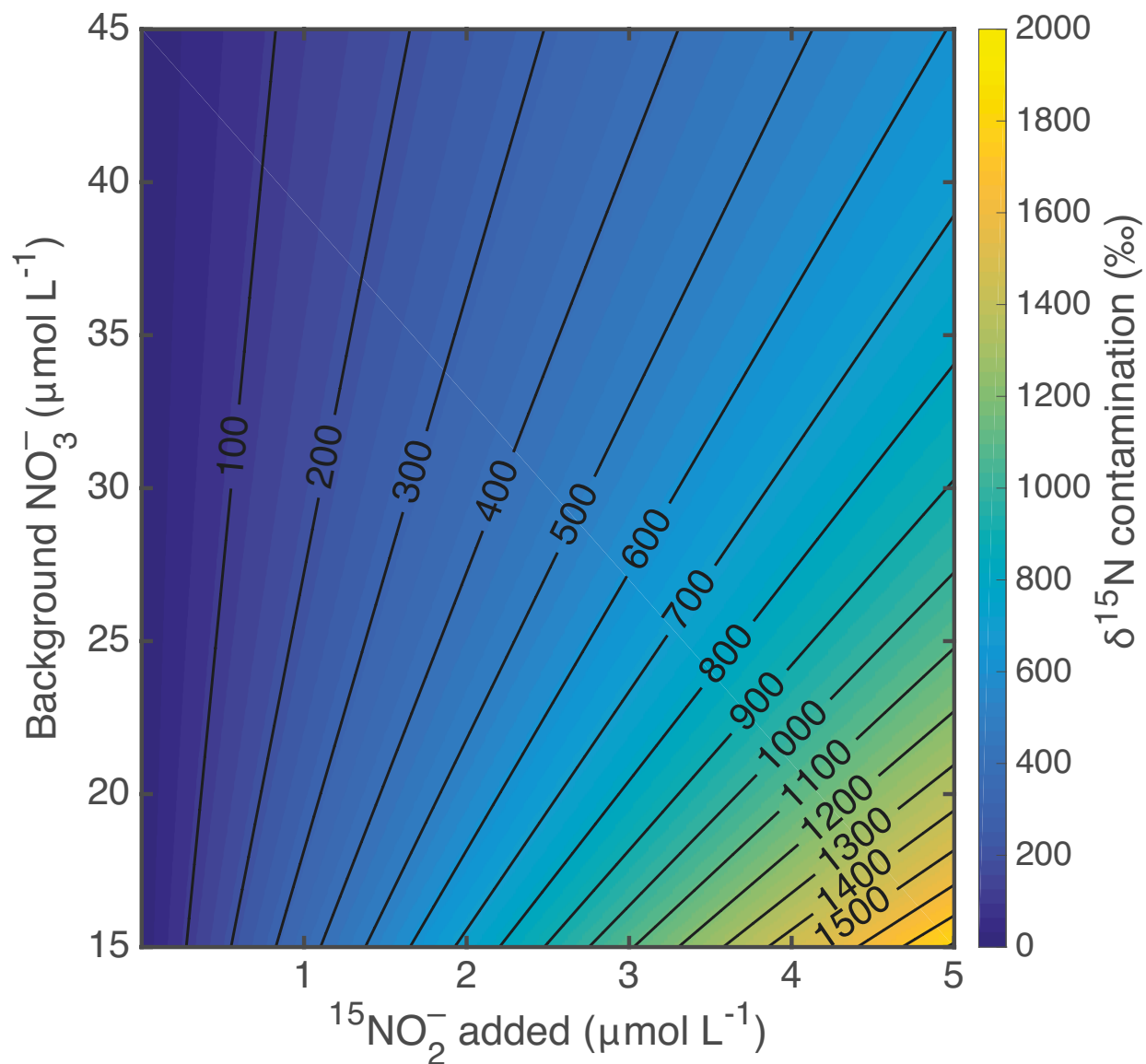[3]Department of Oceanography, Dalhousie University, Halifax, Nova Scotia B3H 4R2 Canada
[4]Department of Geosciences, Princeton University, Princeton, New Jersey 08544, USA

Station	Depth (m)	Nitrate (μM)	Nitrite (μM)	NO₂⁻ oxidation rate (nM/d)			N₂ production rate (nM/d)			NO₂⁻ ox. / N₂ prod.	% anammox	NO₂⁻ ox. from amx (%)[†]
ETNP coastal	25	25.4	0.6	61.7	±	8.3	2.1	±	0.1	28.9	27.0	0.1
	40	21.0	5.9	185.6	±	19.1	56.4	±	5.0	3.3	45.4	1.8
	50	19.0	3.1	158.3	±	21.4	16.4	±	1.1	9.7	79.9	1.1
	60	21.1	6.8	104.3	±	24.4	18.4	±	0.2	5.7	57.1	1.3
	100	17.2	7.5	10.4	±	9.8	11.1	±	0.3	0.9	63.9	8.8
	150	20.5	5.0	11.1	±	7.9	7.1	±	0.4	1.6	64.4	5.3
	250	22.2	2.7	5.7	±	7.5	8.0	±	0.2	0.7	22.8	4.2
	500	33.5	0.0	3.7	±	11.9	7.0	±	0.3	0.5	25.0	6.2
ETNP offshore	90	25.2	0.1	0.0	±	0.0	1.4	±	0.1	0.0	13.0	—
	105	24.3	0.1	45.9	±	6.8	3.1	±	0.3	15.1	39.5	0.3
	115	23.1	0.9	113.4	±	12.4	6.9	±	1.0	16.4	69.8	0.6
	125	21.0	2.7	59.5	±	6.1	9.7	±	1.1	6.2	67.8	1.4
	140	25.7	3.9	4.4	±	18.0	6.4	±	0.5	0.7	53.1	10.1
	150	19.8	6.1	7.3	±	6.6	9.7	±	0.3	0.8	43.2	7.4
	250	27.0	3.0	23.9	±	10.2	3.8	±	0.2	6.4	40.4	0.8
	500	31.4	0.5	5.1	±	3.7	4.4	±	0.3	1.2	40.2	4.5
ETSP coastal	80	11.6	3.3	31.5	±	7.2	12.7	±	1.7	2.5	87.1	4.6
	125	9.9	5.6	11.2	±	2.4	3.8	±	0.6	3.0	64.3	2.8
	150	12.0	7.1	18.2	±	3.0	12.9	±	0.5	1.4	38.4	3.5
	200	15.3	7.0	6.4	±	2.0	8.1	±	0.6	0.8	34.7	5.7
	250	17.6	7.4	5.0	±	3.1	5.0	±	0.2	1.0	40.3	5.1
	280	16.4	6.6	5.7	±	5.3	3.8	±	0.1	1.5	60.7	5.2
	325	21.0	5.6	12.1	±	5.6	3.7	±	0.3	3.3	42.6	1.7
	375	30.7	1.0	29.4	±	6.1	1.5	±	0.0	19.6	63.6	0.4
ETSP offshore	150	19.9	0.0	16.3	±	8.9	0.7	±	0.1	23.3	100.0	0.6
	175	19.7	0.5	33.7	±	5.8	0.6	±	0.2	58.6	100.0	0.2
	200	17.5	5.9	0.0	±	0.0	3.5	±	0.4	0.0	41.6	—
	225	20.1	3.1	7.2	±	2.7	4.9	±	0.0	1.5	41.9	3.7
	250	20.9	7.2	0.0	±	0.0	4.7	±	0.0	0.0	40.9	—
	275	21.2	6.7	0.0	±	0.0	2.2	±	0.0	0.0	48.8	—
	300	28.0	4.3	0.0	±	0.0	1.7	±	0.3	0.0	51.4	—
	350	32.2	1.9	0.0	±	0.0	1.9	±	0.1	0.0	53.8	—

Supplementary Table 1. Nitrite oxidation and reduction to N₂ data. Caption provided on subsequent page.

Supplementary Table 1. Nitrite oxidation and reduction to N$_2$ data. NO$_2^-$ reduction and N$_2$ production rates are mean ± standard error of the slope fit among 15 points. Percent anammox is the amount of N$_2$ production attributed to anammox compared with denitrification. Ratios between NO$_2^-$ oxidation and NO$_2^-$ reduction to N$_2$ from the interior of the ODZs (defined as the lowest O$_2$ measured with no vertical gradient in O$_2$) are highlighted in green. [†]Possible contribution to NO$_2^-$ oxidation by anammox is calculated via the Strous et al. (1998) stoichiometry, whereby 13% of the NO$_2^-$ reduced to N$_2$ is oxidized to NO$_3^-$.

Supplementary Figure 1. Contamination from $^{15}NO_3^-$ in NO_2^- oxidation experiments. The contamination (‰) in initial $\delta^{15}N$ labeling in the NO_3^- pool resulting from 2% contamination (either in the $^{15}NO_2^-$ stock or incomplete removal of $^{15}NO_2^-$ with sulfamic acid) on the basis of $^{15}NO_2^-$ label added and the background NO_3^- concentration is shown in colors and contours.

Supplementary information for:

Nitrite oxidation exceeds reduction and fixed nitrogen loss in anoxic Pacific waters

Andrew R. Babbin[1]*, Carolyn Buchwald[2,3], François M. M. Morel[4], Scott D. Wankel[2], Bess B. Ward[4]

[1]Department of Earth, Atmospheric, and Planetary Sciences, Massachusetts Institute of Technology, Cambridge, Massachusetts 02139, USA
[2]Department of Marine Chemistry and Geochemistry, Woods Hole Oceanographic Institution, Woods Hole, Massachusetts 02543, USA
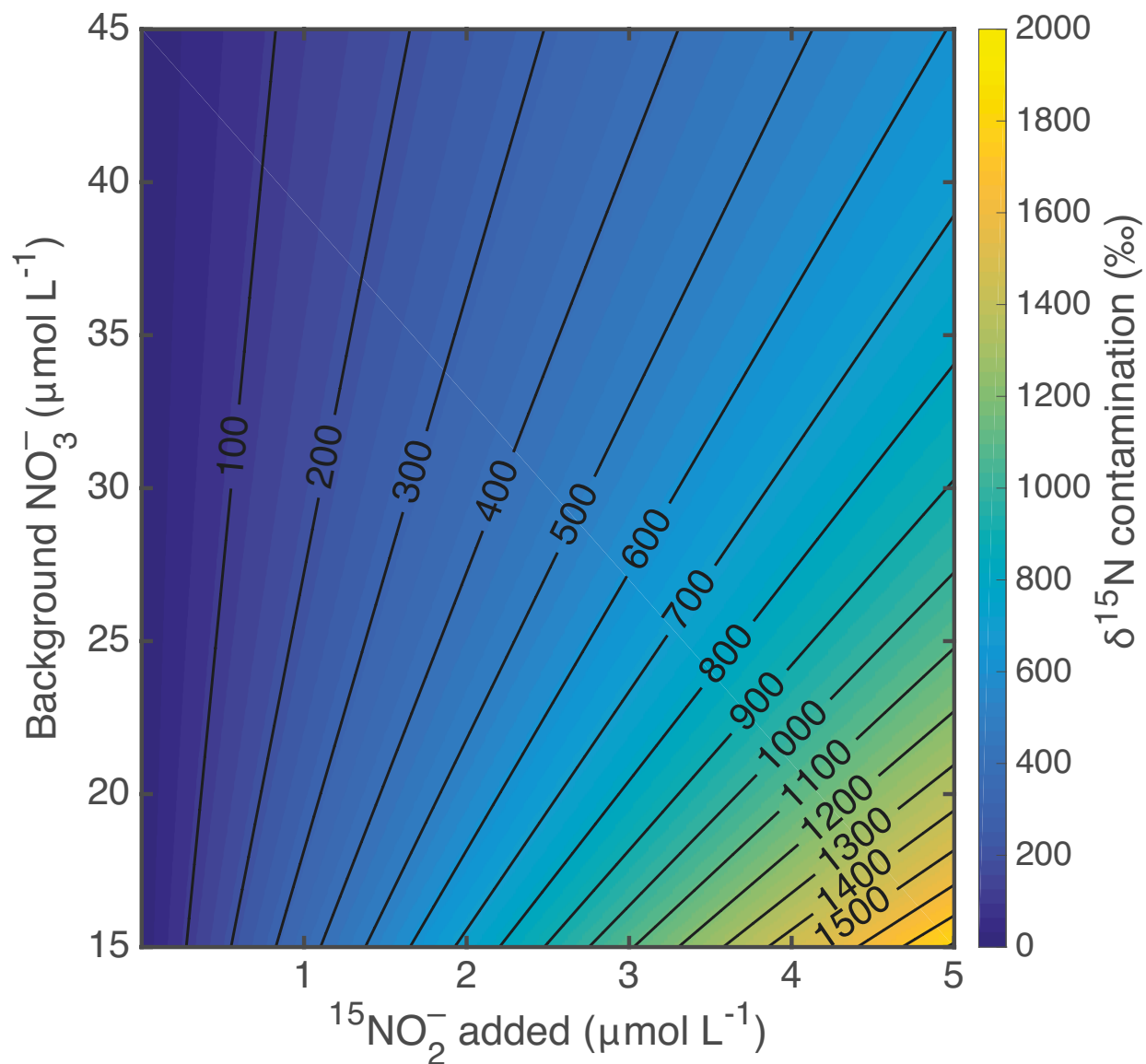[3]Department of Oceanography, Dalhousie University, Halifax, Nova Scotia B3H 4R2 Canada
[4]Department of Geosciences, Princeton University, Princeton, New Jersey 08544, USA

Station	Depth (m)	Nitrate (μM)	Nitrite (μM)	NO₂⁻ oxidation rate (nM/d)			N₂ production rate (nM/d)			NO₂⁻ ox. / N₂ prod.	% anammox	NO₂⁻ ox. from amx (%)[†]
ETNP coastal	25	25.4	0.6	61.7	±	8.3	2.1	±	0.1	28.9	27.0	0.1
	40	21.0	5.9	185.6	±	19.1	56.4	±	5.0	3.3	45.4	1.8
	50	19.0	3.1	158.3	±	21.4	16.4	±	1.1	9.7	79.9	1.1
	60	21.1	6.8	104.3	±	24.4	18.4	±	0.2	5.7	57.1	1.3
	100	17.2	7.5	10.4	±	9.8	11.1	±	0.3	0.9	63.9	8.8
	150	20.5	5.0	11.1	±	7.9	7.1	±	0.4	1.6	64.4	5.3
	250	22.2	2.7	5.7	±	7.5	8.0	±	0.2	0.7	22.8	4.2
	500	33.5	0.0	3.7	±	11.9	7.0	±	0.3	0.5	25.0	6.2
ETNP offshore	90	25.2	0.1	0.0	±	0.0	1.4	±	0.1	0.0	13.0	—
	105	24.3	0.1	45.9	±	6.8	3.1	±	0.3	15.1	39.5	0.3
	115	23.1	0.9	113.4	±	12.4	6.9	±	1.0	16.4	69.8	0.6
	125	21.0	2.7	59.5	±	6.1	9.7	±	1.1	6.2	67.8	1.4
	140	25.7	3.9	4.4	±	18.0	6.4	±	0.5	0.7	53.1	10.1
	150	19.8	6.1	7.3	±	6.6	9.7	±	0.3	0.8	43.2	7.4
	250	27.0	3.0	23.9	±	10.2	3.8	±	0.2	6.4	40.4	0.8
	500	31.4	0.5	5.1	±	3.7	4.4	±	0.3	1.2	40.2	4.5
ETSP coastal	80	11.6	3.3	31.5	±	7.2	12.7	±	1.7	2.5	87.1	4.6
	125	9.9	5.6	11.2	±	2.4	3.8	±	0.6	3.0	64.3	2.8
	150	12.0	7.1	18.2	±	3.0	12.9	±	0.5	1.4	38.4	3.5
	200	15.3	7.0	6.4	±	2.0	8.1	±	0.6	0.8	34.7	5.7
	250	17.6	7.4	5.0	±	3.1	5.0	±	0.2	1.0	40.3	5.1
	280	16.4	6.6	5.7	±	5.3	3.8	±	0.1	1.5	60.7	5.2
	325	21.0	5.6	12.1	±	5.6	3.7	±	0.3	3.3	42.6	1.7
	375	30.7	1.0	29.4	±	6.1	1.5	±	0.0	19.6	63.6	0.4
ETSP offshore	150	19.9	0.0	16.3	±	8.9	0.7	±	0.1	23.3	100.0	0.6
	175	19.7	0.5	33.7	±	5.8	0.6	±	0.2	58.6	100.0	0.2
	200	17.5	5.9	0.0	±	0.0	3.5	±	0.4	0.0	41.6	—
	225	20.1	3.1	7.2	±	2.7	4.9	±	0.0	1.5	41.9	3.7
	250	20.9	7.2	0.0	±	0.0	4.7	±	0.0	0.0	40.9	—
	275	21.2	6.7	0.0	±	0.0	2.2	±	0.0	0.0	48.8	—
	300	28.0	4.3	0.0	±	0.0	1.7	±	0.3	0.0	51.4	—
	350	32.2	1.9	0.0	±	0.0	1.9	±	0.1	0.0	53.8	—

Supplementary Table 1. Nitrite oxidation and reduction to N₂ data. Caption provided on subsequent page.

Supplementary Table 1. Nitrite oxidation and reduction to N$_2$ data. NO$_2^-$ reduction and N$_2$ production rates are mean ± standard error of the slope fit among 15 points. Percent anammox is the amount of N$_2$ production attributed to anammox compared with denitrification. Ratios between NO$_2^-$ oxidation and NO$_2^-$ reduction to N$_2$ from the interior of the ODZs (defined as the lowest O$_2$ measured with no vertical gradient in O$_2$) are highlighted in green. [†]Possible contribution to NO$_2^-$ oxidation by anammox is calculated via the Strous et al. (1998) stoichiometry, whereby 13% of the NO$_2^-$ reduced to N$_2$ is oxidized to NO$_3^-$.

Supplementary Figure 1. Contamination from $^{15}NO_3^-$ in NO_2^- oxidation experiments. The contamination (‰) in initial $\delta^{15}N$ labeling in the NO_3^- pool resulting from 2% contamination (either in the $^{15}NO_2^-$ stock or incomplete removal of $^{15}NO_2^-$ with sulfamic acid) on the basis of $^{15}NO_2^-$ label added and the background NO_3^- concentration is shown in colors and contours.